HYDRODYNAMIC DRAG REDUCTION

IN AQUEOUS POLYMER SOLUTIONS

THE INFLUENCE ON HYDRODYNAMIC DRAG OF HIGH MOLECULAR WEIGHT COMPOUNDS IN THE TURBULENT BOUNDARY LAYER

by

JOHN RICHARD SMALLMAN, B.A.Sc.

A Thesis

Submitted to the Faculty of Graduate Studies

in Partial Fulfilment of the Requirements

for the Degree

Master of Engineering

McMaster University

May 1967

MASTER OF ENGINEERING (1967) Mc.MASTER UNIVERSITY

(Mechanical Engineering) Hamilton, Ontario.

TITLE: The Influence on Hydrodynamic Drag of High Molecular Weight Compounds in the Turbulent Boundary Layer

AUTHOR: John Richard Smallman, B.A.Sc.(University of Toronto)

SUPERVISOR: Doctor J.H.T. Wade

NUMBER OF PAGES: viii, 105

SCOPE AND CONTENTS:

This thesis describes in detail an experimental study made into the evaluation and explanation of the reduction in hydrodynamic drag resulting from the addition of small proportions of certain water soluble polymers to distilled water.

An experimental apparatus was designed which would, it was hoped, yield repeatable results. This apparatus consisted basically of a chamber which was filled with the test fluid, and which contained a rotating disk whose speed could be varied and whose torque could be measured.

To develop a theory which would explain this reduction in hydrodynamic drag a boundary layer velocity profile was determined for pure water at a given disk radius, and then for water containing the long chain polymer "polyacrylamide MRL-159". These two velocity profiles were determined using a special velocity probe developed for the purpose; and hence a section of this thesis will describe in detail its development and operation.

All solution concentrations alluded to in the text, in the tabular and graphical presentations, and in the calculations are in parts of solute per million parts of solvent (P.P.M.), by weight.

The weights of the solutes used in the determination of concentrations were corrected for moisture content as determined in oven drying procedures fully described in section 4.2 entitled "Stock Preparation and Control".

ACKNOWLEDGEMENTS

The author wishes to thank Dr. J.H.T. Wade, under whose guidance this research was carried out, for the assistance and advice given by him throughout the course of the project.

The assistance given by Dr. J.O. Medwell, especially in the development of the velocity measuring equipment described in this thesis was greatly appreciated by the author.

The literature and polymer samples supplied free of charge by Stein-Hall Limited of Westhill, Ontario, Charles Tennant and Company (Canada), Limited of Weston, Ontario, and the Hercules Powder Company of Burlington, Ontario; as well as the many informative telephone calls exchanged with Mr. Alan A. Risdon, Technical Sales Representative of Stein-Hall Limited, are also gratefully acknowledged.

This research was supported financially by the National Research Council of Canada, Ottawa, under grant number A-1585.

TABLE OF CONTENTS

APPENDIX

LIST OF FIGURES

1. INTRODUCTION

The addition of small quantities of certain natural and synthetic polymers to water to form a solution has been observed to reduce the hydrodynamic drag to a large extent. This phenomenon is a topic of interest to those engaged in hydrodynamic model testing, and especially in the testing of ship's models in towing tanks. The drag characteristics of the water in these tanks vary slowly with time, making it difficult to interpret the results of this testing. As a result, some simple and rapid method of determining the variation in drag from day to day is required. Presently most tanks have a standard model, and use it to calibrate the drag characteristics of the water before each model test. However, this is a time-consuming procedure.

Further, it is hoped that when better analytic or experimental methods are available to predict the effects of long chain polymers used in model tests to ship and submarine hulls, that these polymers will also prove to be an economically feasible way to increase the speed of such vessels while reducing their drag.

Companies involved in the transfer of water over long distances, and especially those located in remote areas, are interested in the increase in capacity and decrease in operating costs of pumping systems which could be brought about by adding these substances to water, and probably to other liquids which have to be transferred great distances by pipeline. It is probable also that a reduction in boundary layer thickness which occurs with the addition of these polymers to water could be of interest to those investigating heat transfer phenomena.

The first part of the experimental work in this thesis is concerned with developing curves of drag reduction as a function of solution concentration for the most effective polymers tested. Emphasis has been placed upon accounting for all the variables which could affect the drag reduction, either by controlling them or by determining a suitable method of accounting for them. It is considered that these results will be, therefore, useful in that the test methods could be repeated at any time, and similar results would be obtained.

The second part of the experimental work reported in this thesis involved obtaining velocity profiles in the boundary layer of the primary flow regime (i.e. orthogonally outwards from the face of the rotating disk) and, with these velocity profiles, showing that one of the theories on the mechanism of drag reduction is almost certainly correct.

2. LITERATURE SURVEY

The reduction in hydrodynamic drag occasioned by the addition of trace quantities of certain long chain polymers to water has been the subject of some investigation over the past few years. The phenomenon has been observed since the late nineteenth century in towing tanks used for testing ship models. Hoyt and Fabula (1)[#] cite the example of the random variation reported in the "resistance quality of the water" from 1887 to 1956 in the towing tank at Haslar, England which was reduced from its initial value at times by as much as 14%. It was shown by chemical and biological analysis that no significant changes had taken place in the water.

Toms (3) investigated the Non-Newtonian flow characteristics of the polymer polymethyl methacrylate in the organic solvent monochlorbenzeme at concentrations up to 3% (30,000 P.P.M.) using a pipe flow loop as a test apparatus. He discovered, using a modification of the Reynolds colour filament technique, that a Reynolds Number of 2,000 still defined the beginning of the regime of transition from laminar to turbulent flow, despite the strongly Non-Newtonian characteristics of the solution. Further, he observed from his experiments that an increase in the rate of flow at a constant fluid source pressure occurred at increased polymer concentrations only if the flow was turbulent.

Dodge and Metzner (10), using dye injection studies and short duration flash photography techniques, suggest that the formation of

---

Numbers in brackets designate references. See chapter 12 entitled "References".

horseshoe vortices generated close to the wall of the pipe are strongly suppressed from propagating outwards due to the increasing viscosity in that direction. This viscosity gradient results from the pseudoplastic characteristic of inverse shear rate with viscosity.

The rotating disk apparatus for measuring the drag reduction as a function of the polymer concentration has been used by Hoyt and Fabula (1) as well as by Hamill (5). However, conclusions drawn by them as to the mechanism of the drag reduction in very dilute polymer solutions were not supported by their experimental data. These reports are of particular interest, nevertheless, because the type of apparatus used in them, as well as some of the types of polymers, and the range of concentrations are quite similar to those reported in this thesis.

Merrill, Mickley, Ram and Stockmayer (6) refer to the probability of degradation by shear of the long chain polymer molecules contained in a solution. They place particular emphasis on the care which must be taken in preparing the solutions, suggesting that a slow, gentle mixing process should be employed. However, in making aqueous solutions of these polymers, violent agitation is required for a short time until the solution has formed, and, it would be extremely difficult to evaluate the degradation in the drag reducing tendency of these solutions which has occurred as a result of this phase of the mixing process.

Simha and Zakim (7) describe the randomly coiled nature of the type of long chain polymers used in this research, namely, flexible,

non-associating, free-drawing, linear polymers[#]. They also introduce a theory with supporting experimental evidence on the inverse variation of the randomly coiled diameter of the polymer molecule with solution concentration. This phenomenon may help to account for the relatively high drag reducing capability of very weak polymer solutions.

Kaufmann (8) develops the necessary relationships to calculate the manometric head induced by an interface between two fluids. He also lists an experimental value for the surface tension in pounds force per foot between water and air. These relationships were based on the assumption that the interface was subtended on an element of circular cross-section, whose diameter was sufficiently small that the shape of the interface could be approximated by the curved surface of a spherical segment of one base[##]. Using these relationships, due allowance could be made in the calculations contained in this thesis for the air-water interfaces encountered with the velocity measuring apparatus.

Some association of these polymers with the hardness ions in plain tap water has been brought to the author's attention in personal correspondence with the Charles Tennant Company Limited.

Values of capillary head calculated using this assumption were found to agree exactly with values experimentally observed, to within the precision allowed by the standard U-tube manometer.

3. EXPERIMENTAL APPARATUS

The apparatus used in this experimental work is shown in figures 1A to 2, and was, in effect divided into two distinct parts. The main testing facility, containing all the instrumentation, is shown in figures 1A and 1B, and a part of the batch preparation facility is shown in figure 2. The remainder of the batch preparation facility is described fully in section 3.2, entitled "Batch Preparation Facility".

3.1 The Main Testing Facility

In this discussion of the main testing facility, capital letters in parentheses refer to the elements of this facility as designated in figures 1A and 1B.

3.1.1 The Test Chamber (A)

The test chamber consisted of a cylindrical vessel aligned with its axis in a horizontal plane. It was completely open at one end, and had a centered orifice in the other end in which a rotating shaft was located. A tapered sleeve, part of which was an integral section of the vessel, projected into it from the shaft end. It contained two tapered roller bearings, in reverse alignment to each other to absorb radial and axial loads, a lip type dynamic shaft seal, and an o-ring seal. This sleeve had a removable end so that the shaft could be withdrawn for inspection without dismounting the roller bearing cups.

The inside diameter of the cylinder was approximately 14¼ inches, and was honed and nickel plated so that the maximum root mean square roughness was two microinches (μ inch). As a result the cylinder was hydrodynamically smooth and also corrosion resistant.

There were two thick webs, one on each side of the cylinder, parallel to the centreline and horizontally aligned, welded on the outside. They were provided with boltholes, and tapered holes for dowel pins, by means of which the chamber was located and supported. These webs were welded in place before the inside diameter was honed and nickel plated so that no distortion to the inside diameter would occur as a result of thermal stresses. The chamber was also provided with an overflow pipe and valve at the upper extreme, on the periphery.

A disk, also nickel plated , and with a peripheral o-ring seal fitted into the open end of the housing and could be moved back and forth by means of a small anti-backlash jack (B). This disk also had an eccentric hole in which the velocity probe traversing mechanism (C) was mounted by means of quick releasing clamps. There were two tapped holes in the fixed end of the chamber into which pipes were threaded for the fluid circulating system.

3.1.2 Rotating Disks and Drive

The rotating disks were manufactured from stainless steel plate, three sixteenths of an inch in thickness. In all, two disks were used, one being ten inches in diameter, the other being twelve inches in diameter, both with root mean square roughness of less than twenty

microinches (μ inch). This low roughness level was maintained to ensure hydrodynamic smoothness. The disks were mounted on the rotating shaft by means of keyed hubs. The axial and radial spacing provided between the disks and the main chamber were large enough to ensure operation of the system as a free disk apparatus, or, in a hydrodynamic sense, to ensure that the disk could not "see" the chamber (Section C, Appendix). The shaft was $\frac{3}{4}$ inch diameter cold rolled steel, and a flexible coupling driven by a D.C. motor was keyed to the end of the shaft outside the main chamber. The shaft and hubs were also nickel plated.

The 200 volt, $\frac{1}{2}$ horsepower D.C. motor (D) was mounted by means of roller bearing races so that the motor cage was free to rotate#. These bearing races were mounted to the motor cage rather than to the motor shaft so that they generated no dynamic friction which would appear as a contribution to the dynamometer error. The motor was restrained from free rotation by an arm and a spring balance (E), and was used thus as an electric dynamometer. The speed of the electric motor could be varied by means of a rheostat (F) connected in series with the armature.

3.1.3 The Fluid Circulating System

The fluid was constantly circulated by means of a centrifugal pump (G). The pump had an open, unshrouded type impeller, and ran

---

All electrical equipment used on the test facility was grounded, and was provided with starters and overload protection relays.

at the comparatively low speed of approximately 580 R.P.M. so that the shear stresses and turbulence levels were minimized. The pump was driven by a $\frac{1}{2}$ horsepower A.C. induction motor running at 1750 R.P.M., speed reduction being accomplished by a vee belt drive. A teflon shaft seal was provided so that no contamination of the fluid occurred at the pump stuffing box.

The piping was arranged so that the fluid was circulated through the main chamber and the temperature control vessel in series. Valves were arranged so that the temperature control vessel or the pump could be partly or wholly bypassed. Drain lines with valves were provided at all low points in the system.

3.1.4 The Temperature Control Vessel (H)

In this vessel a constant cooling rate, constantly operating refrigeration coil was immersed (I), as well as a constant heating rate, intermittently operating heating coil (J). The heating coil cycles were controlled by temperature monitoring of the test fluid. This "buffeting" type of temperature control is presently considered to minimize the temperature fluctuations within the fluid better than, for example, a temperature regulated refrigerator operating alone.

A stirrer was also provided which constantly agitated the fluid. The vessel itself was of cylindrical shape, its axis being vertically aligned. The fluid was open to atmosphere at the top, and the vessel was hence used for level control as well as being the place where test fluid was let into the fluid circuit. The vessel was manufactured from four inch diameter, thick wall commercial copper tubing and $\frac{1}{4}$ inch copper plate.

3.1.5 The Transfer Pump (K)

A one hundredth horsepower centrifugal pump with mechanical shaft seal was used to transfer the test fluid from the preparation bins to the testing system. It was equipped with flexible hoses, a small hand primer, and a plug type valve on the downstream side of the pump.

3.1.6 The Air-Ejecting Probe Control Panel (L)

This section of the main testing facility is fully discussed in section 3.3 entitled "Velocity profile measuring apparatus". The control panel was essentially a mounting board for the valves associated with the velocity probe system.

3.1.7 Measuring Equipment

The speed of the rotating disk was measured with an electric tachometer comprised of an electric generator and voltmeter which had been calibrated as a matched set. The tachometer generator was driven by a unity speed ratio timing belt from the disk shaft. The timing belt ensured perfect synchronism between the disk shaft and the tachometer generator rotor. The tachometer generator was of the alternating current type, so that reversal of the direction of rotation of the disk would not affect the speed readout voltmeter. The voltmeter was graduated from 0 to 2,000 R.P.M. in increments of 20 R.P.M.

The dynamometer load was measured with a 0 to 1 pound range spring balance, graduated in 0.01 pound increments. Higher loads were measured by applying two weights at a certain moment arm on the side of the disk driving motor remote from the dynamometer scale,

which effectively added to the 0 to 1 pound range two further ranges of 1 to 2 and $1\frac{1}{2}$ to $2\frac{1}{2}$ pounds.

The temperature of the test fluid was read with a mercury in glass thermometer immersed in the temperature control vessel, and graduated in increments of 2 Fahrenheit degrees.

The position of the boundary layer velocity measuring probe was determined using a traversing mechanism graduated in thousandths of an inch, and which was probably accurate to about 2 or 3 thousandths of an inch. This traversing mechanism was driven by a machined screw thread, operated in such a way that backlash of the screw mechanism would not appear as an error in the measurements.

A high quality Swiss stopwatch was used for all the time measurements.

The weigh scales used in the preparation of the test solutions are alluded to in section 3.2, entitled "Batch Preparation Facility".

The calibration of the tachometer was verified using a hand held mechanical revolution counter and stopwatch. The calibration of the dynamometer spring balance was verified by loading it with standard weights.

3.1.8 The Superstructure

The framework of the main test facility was constructed from $\frac{3}{4}$ inch, square cross-section steel tubing, all members being gas welded. The base for the main chamber, jack support, and D.C. motor support was made from steel plate, 7/16 of an inch thick, strengthened by welding a rectangular array of channel members on its underside.

Horizontal reference planes were milled at strategic points on the base as a reference for the alignment of the jack, main chamber, and D.C. motor. The base was then lowered onto the framework where the channel members served to locate the base in the aperture in the top of the framework. The base was mounted in this way so that it could be removed at any time, and replaced on a milling machine to check the alignment.

3.2 Batch Preparation Facility

The batch preparation facility was composed of the following pieces of equipment:

(i) Analytical balance, used for determining the weights of the polymer samples.#

(ii) Refractory lined furnace, used in the determination of the moisture content of the polymer samples.

(iii) Small beam scales, for weighing the distilled water used in the preparation of concentrated stock solutions.

(iv) Variable speed electric agitator, used for agitation of concentrated stock solutions as polymers were added gradually to the water.

(v) Large beam scales, on which distilled water was weighed for the preparation of the low concentration batches of test solutions, in hundred pound lots.

All polymer samples obtained were in powder or fine granular form, essentially free-flowing.

(vi) Holding drums with triple, watertight, polyethylene liners, used for storing the test solutions. Standard zinc dipped garbage cans were used, with polyethylene bags for liners. Three bags minimized the possibility of leakage. These drums were provided with special wooden covers, upon which were mounted variable speed, air powered stirrers.

(vii) Watch glasses, upon which the polymer samples were weighed, and stainless steel tools for handling the polymer samples.

3.3 Velocity Profile Measuring Apparatus

The velocity profiles were measured with a modified stagnation probe, and U-tube manometers made from precision glass, one using water, the other using mercury for a manometric fluid. Velocity heads in excess of three feet of water were measured using the mercury filled U-tube manometer.

In this modified stagnation probe, high pressure air was introduced as an intermediate fluid between the manometric and test fluids, via a very fine metering valve. During this time the main chamber was acoustically monitored using a sensitive stethoscope and, when the bubbles could be heard breaking off the tip of the probe, the high pressure air supply was cut off. When the bubbling had ceased, a remarkably steady manometric head reading was noted on the manometer. The portion of this manometric head which was due to the static pressure

was measured with a simple static tube mounted on the test chamber[#], and that due to the interface pressure could be accurately calculated, hence the velocity head could be determined. This type of velocity probe has consequently been called an "air-ejecting dynamic probe".

Provision was made in this apparatus for using a modified Pitot Tube having both static and stagnation orifices (figure 16), so that further research could be conducted with the apparatus in which more precise and quantative velocity profiles could be measured. In the context of this thesis, the velocity profiles are chiefly qualitative (figure 14).

A fast acting valve which would communicate the pressurized air loop of the velocity probe system with the atmosphere was included to avoid the possible spilling of manometric fluid should the high pressure air supply valve be opened too far. (Figure 4, "Pneumatic Schematic")

The probe used in this experiment was made from 25 gauge stainless steel hypodermic tubing, with an inside diameter of 0.0095 of an inch. The tip of the probe, which faced the tangential component of velocity was $\frac{3}{4}$ of an inch long, and lay in a horizontal plane.

This pressure measurement should be the same as the static pressure at any point on the disk, since the disk is immersed in a "hydrodynamically large" expanse of fluid, and is wetted on both sides (12).

4. EXPERIMENTAL PROCEDURE

Whereas the Experimental Apparatus (Chapter 3) was discussed in order of importance, the Experimental Procedure can be most logically covered in the same chronological order as is required in the actual experimentation.

4.1 Verification of Measuring Apparatus

In order to verify the accuracy of the measuring apparatus, a test run was undertaken to obtain values of dimensionless drag coefficient at different Reynolds Numbers. Although a small range of disk speeds was employed (from 1150 R.P.M. to 1400 R.P.M.), and thus a small range of Reynolds Numbers resulted, close agreement with the theory and with other experimenters' data was observed. The experimental values thus obtained were close to those cited in N.A.C.A. Report Number 793, which used air as a test fluid (9). Hoyt and Fabula (2) mention that if the data lies between the Von Karman and Goldstein relations for unshrouded disks, then the accuracy of the torque measuring device is adequate (figure 5). It is therefore reasonable to assume that the dynamometer and tachometer are sufficiently accurate, and that the free disk assumption is valid.

The disk used in this section of the experimental work was approximately 9.85 inches in diameter, and 0.2 of an inch thick. Allowance was made for the hydrodynamic drag on the rim of the disk by adding the disk thickness to the disk diameter, and using this

new value for all calculations involving the radius or diameter of the disk. A subscript (e) will be used to denote that the radius or diameter being referred to is that of the disk expanded thus in diameter by the disk thickness.

4.2 Stock Preparation and Control

As all of the polymers used in this experiment were hygroscopic, great care was taken to keep all of the sample containers tightly closed, and to open them for a minimum of time during the removal of quantities of polymer. Although stock solutions were only prepared on two occasions, judicious choice was made of the time of preparation of the second series to match the room temperature and relative humidity which existed during the preparation of the first series as closely as was practicable (within one Fahrenheit degree and 3% relative humidity).

The following polymers were tested in the experiments. However, the first three were found to produce no significant drag reduction in dilute aqueous solution. Consequently, only the test results of the latter five polymers were reported in this thesis.

ALGINATES (Supplied by Charles Tennant and Company.)

Marex

Superloid

BEAN DERIVATIVES (Supplied by Stein-Hall Limited.)

Locust Bean Meal

Guar Bean Gum J2S1

Guar Bean Gum A-20-D

POLYACRYLAMIDES (Supplied by Stein-Hall Limited.)

MRL-19

MRL-159

MRL-295

All of these substances were in fine granular or powder form. Some grains of the polyacrylamide MRL-19 were observed to fly off the weighing pan spontaneously, probably due to an electrostatic charge built up in them as a result of being handled with plastic utensils. Thereafter, all handling of the polymers was carried out with stainless steel utensils.

The moisture content of each sample was determined by weighing the sample, and re-weighing it after each of several baking operations. These baking operations consisted of placing the samples in a refractory furnace for four hours at a temperature of 150 degrees Fahrenheit for the alginates, and for two hours at a temperature of 220 degrees Fahrenheit for the bean derivatives and the polyacrylamides, the times and temperatures having been suggested by the manufacturers#.

Stock solutions were then made of 4,000 P.P.M. (except in the case of the polyacrylamide MRL-295, whose stock concentration was chosen as 2,000 P.P.M. due to exceptionally high stock solution viscosity) by slowly adding the polymer to the eye of the vortex formed in the water by a rapidly rotating agitator. These stock solutions, based on the oven dried weight of the polymers, were made up in five pound lots, and stored in polyethylene containers, tightly stoppered.

Moisture contents are tabulated in the Appendix, Section A.

4.3 Batch Preparation and Control

The test solutions were subsequently made up in 100 pound lots by adding stock solution to distilled water in the required proportions. These solutions were constantly agitated with low pitch, air powered stirrers running at speeds of 120 R.P.M. to 150 R.P.M. for at least two days so that, even in the lowest concentration solution, all concentration gradients would be dissipated. Stock solutions and test solutions were systematically labelled so that all preparation details of any given solution could be accounted for.

4.4 Batch Transfer and General Test Procedure

In order to determine that portion of the dynamometer load which was due to bearing and seal friction, as well as frictional resistance between the disk shaft and the test fluid, a test run was undertaken in distilled water with the disk and hub removed. Thus, a dynamometer error of 0.05 foot-pounds was observed which varied only slightly over the range of test speeds (1200 R.P.M. to 1450 R.P.M.). This error remained unchanged when the main chamber was emptied of test fluid; and thus it was concluded that the portion of the dynamometer error resulting from the frictional resistance between the test fluid and the disk shaft was negligible.

As a consequence the torque correction of 0.05 foot-pounds was independent of the polymer concentration of the test fluid, and was applied to all torque measurements. Furthermore, since this small torque error would appear on both the numerator and denominator of the drag reduction expression, it probably need not even be applied.

4.4.1 Torque Measurement

In these series of tests, in which torque was measured as a function of both disk speed and polymer concentration, the tests were always undertaken in order of increasing polymer concentration. The test equipment was thoroughly purged before each test.#

In each test the hydraulic circuit was filled with the test fluid until the overflow tubes on the circulating pump and on the main chamber had begun to pass test fluid. The overflow valves were then closed, and the filling was continued until the test fluid was at a level of one inch below the top rim of the temperature control vessel. When the circulating pump was started any small bubbles of air which might have remained in the pipeline or elsewhere, would rise either to the top of the main chamber, where they could be exhausted by opening the overflow valve briefly, or directly to atmosphere via the free surface of the temperature control vessel.

The drag reduction tests themselves were undertaken as follows: After the apparatus had been filled with the test fluid the valves on the hydraulic circuit were operated in such a manner that the circulating pump bypass was fully open. The temperature control vessel bypass valve was fully closed, as were the drain and overflow valves. All other valves were fully open. In short, two fluid loops in parallel were being operated by the circulating pump:

Justification of this testing order, and details of the purging procedure are described in section 4.6 entitled "Discussion of Contamination Control".

one loop being a direct pipeline from the pump exit to the pump intake, the other loop containing the main chamber and the temperature control vessel in series. This valving pattern allowed the fluid to be circulated with a minimum of turbulence.

The temperature control apparatus was then set to the required temperature of 86 ^{o}F., using the conversion chart developed for the purpose which relates the setting numbers on the apparatus to temperatures in degrees Fahrenheit (figure 15).

The disk driving motor was then set into operation, and regulated to 1,200 R.P.M., and immediately thereafter the circulating pump and stopwatch were started. It was generally found that the system required about twelve minutes to come to thermal stability, and therefore a warm up time of twenty minutes was selected.

At twenty minutes elapsed time, the disk speed was set at 1,150 R.P.M., the dynamometer scale was levelled to the reference mark at which it had been zeroed, and a reading was made of the dynamometer load. At intervals of ninety seconds, further readings were taken of the dynamometer load, each one with a speed increase of 50 R.P.M., until a load reading had been made for 1,500 R.P.M. The readings were then repeated as the 50 R.P.M. speed increments were subtracted until 1,150 R.P.M. was again reached. This process was then repeated so that for every speed setting there were four torque load readings. The end readings, corresponding to speeds of 1,150 R.P.M. and 1,500 R.P.M. were then discarded, leaving a set of six speed settings, each having four related dynamometer load values.

Thereafter, all electrical equipment was shut down, and drains were opened on the pipeline system, the circulating pump, and the temperature control vessel. Due to the location of the inlet and outlet pipes in the main chamber, the chamber would still be about half full of the test fluid. The bulk of this fluid was then drawn off with the flexible intake line of the transfer pump through the handhole provided for the mounting of the velocity probe. The moveable end plate of the main chamber was then withdrawn, allowing the remainder of the test fluid to spill out into a small drain trough, and thence to the drain. The zero setting of the dynamometer scale was then re-checked for accuracy. Following this, the test facility was purged, and the complete procedure was repeated for all other solution concentrations of the same polymer.

The complete procedure for each polymer was then given a batch number, and cross references were kept so that all details as to the nature and origin of any batch, including the details of stock solution and test solution preparation could be referred to if necessary. The maximum temperature variation noted during the tests was plus or minus 0.5 ^{o}F. from the test fluid temperature of 86.0 ^{o}F. The final results of these tests are portrayed in graphical form in figures 6 to 11 inclusive, and in tabular form in Section A of the Appendix.

4.4.2 Time Rate of Torque Variation Measurement

For this portion of the experimental work, a fixed disk speed of 1,250 R.P.M. was chosen as being almost equal to the time average overall speed in the drag reduction tests of 1,268 R.P.M. Only the polyacrylamides MRL-159 and MRL-295 were selected to be tested

for time dependence of drag, as they were the most effective drag reduction additives, and also as a noticeable increase in torque was observed for successive readings at the same disk speed during the drag reduction evaluation tests.

These two polyacrylamides were tested in concentrations of 50 P.P.M. A test was also undertaken with distilled water to ensure that no variation in the torque measurements occurred as a function of time when no polymers were present.

At zero time the circulating pump, temperature control apparatus and disk driving motor were started up, and dynamometer load readings were taken every two minutes. The laboratory had been intentionally warmed up to 84 ^{o}F. so that the testing temperature of 86 ^{o}F. was attained within three minutes of starting up. Hydraulic circuit valve settings, system purging and system draining procedures were identical to those described in section 4.4.1 entitled "Torque Measurement".

Evaluation of these time effects showed them to be significant and, when applied to the drag reduction results in the form of correction factors, they altered the results very considerably (figures 12 and 13).

4.5 Velocity Measuring Test Procedure

In order to minimize the time rate of torque increase which is due to the degradation by shear of the polymer, the circulation pump and temperature control apparatus were not used in this phase of the experimental work. A lower disk speed of 825 R.P.M., a larger disk diameter of twelve inches and the relatively short

duration of the tests (about ten minutes) made it possible to determine the necessary experimental points for one velocity profile while incurring only one degree Fahrenheit temperature rise.

The tangential velocity profile in the boundary layer was evaluated at a radius of $5\frac{1}{2}$ inches, the traverse starting close to the disk and moving outwards orthogonal to the face of the disk in increments of five thousandths of an inch, until at least two successive identical manometric heads were observed. The experimental point closest to the rotating disk was that at which the probe could be heard lightly contacting the face of the disk. The true probe position corresponding to this velocity head reading was taken as being ten thousandths of an inch removed from the surface of the disk, that is, removed from the surface by a distance equal to the outside radius of the probe.

The boundary layer thickness and free stream velocity were evaluated at the first experimental point after which no further manometric head change occurred, and these values were used to render dimensionless the distance and velocity values within the boundary layer (figure 14).

4.6 Discussion of Contamination Control

In dealing with very low concentration solutions of a substance, extreme care must be exercised to ensure that the test system be clean.#

In this context a clean system is one in which any traces of contaminant present in the system are not only small in quantity, but also closely matched in drag characteristics to the incoming test solution.

The procedure followed in avoiding contamination was composed of three essentially different precautions:

(i) Before a new batch of test solution was placed in a storage bin, the three polyethylene liners were removed from the bin, and new liners inserted.

(ii) The hydraulic circuit of the main test facility was purged after each run. This purging consisted of partially filling the hydraulic circuit with distilled water, running the circulating pump for a period of two or three minutes, and then emptying the circuit. The circuit was subsequently rinsed down with some of the solution next to be tested, which was then emptied also. As a consequence, any moisture remaining in the circuit of the main test facility would almost match the incoming test fluid in concentration, and in genus. The system could therefore be considered to be as clean as possible.

(iii) The fluids were tested in order of increasing solute concentration. Thus, even if some of the previous test fluid were not removed by the purging process, its effect on the incoming test fluid would be minimized.

To verify that the solutions were indeed of the concentrations expected, a carbon content analysis of three concentrations of Guar Gum J2S1 was undertaken by the Civil Engineering Department at McMaster University. The concentration in P.P.M. of carbon was predicted by multiplying the concentration of the test solution by the fraction by weight (Mole Fraction) of carbon within an individual Guaran unit (11). (Guaran is the term used for the

basic molecular unit found repeated many thousands of times in a typical molecule of Guar Gum.)

The carbon concentrations of the test solutions as reported by the carbon content analyzer were corrected to allow for the carbon content of the distilled water. The experimental and calculated carbon content values thus obtained matched each other to within the accuracy expected of the carbon content analyzer. (The accuracy would be at best plus or minus 10% in this case, so that only very gross errors would be detected by this verification procedure.)

5. DEVELOPMENT OF VELOCITY MEASUREMENT APPARATUS

The development of a somewhat original velocity measurement apparatus was required because of the combination of two experimental difficulties inherent in experimentation with disks rotating in a fluid whose shear characteristics are time dependent. In the first place, the boundary layer developed in water on a rotating disk is quite thin. In this case, a twelve inch diameter disk rotating at 825 R.P.M. would develop a boundary layer only 136 thousandths of an inch in thickness at the outer disk radius of approximately six inches. It was further discovered that a 50 P.P.M. solution of the polyacrylamide MRL-159 had a boundary layer thickness less than half of that for water.

In the second place, the shear characteristics of the solutions being tested are time dependent, therefore, the velocity profile in the boundary layer is also time dependent. The way in which the velocity profile in the boundary layer would change with time depends upon the mechanism by which the addition of the polymer to water affects the flow phenomena which occur within the boundary layer. The effect of the polymers is reduced because their molecular structure is broken down as a function of the length of time that they are subjected to shear. Consequently, the boundary layer would tend to become more nearly similar to that for pure distilled water as the testing time increased.

Were it not for the time dependence aspect of the test fluids being investigated, a common Pitot Tube connected to a straight

manometer might be used for the measurement of velocities. However, as a very small Pitot Tube would have to be used in such a thin boundary layer, the time required for the measuring apparatus to reach stability would be too great. If, for instance, each reading required thirty minutes to reach stability (probably a low assumption) and six readings were taken, the elapsed time of three hours during which the test fluid had been subjected to shear would be sufficient to change markedly the properties of the fluid during the course of the test.

Had the boundary layer not been so thin, hot film anemometry might have been used to measure the velocities. However, hot film probes are large and blunt, and could not be used as a velocity measuring device in this experiment where a minimum of disturbance in the boundary layer is essential.

The requirements were indeed for an apparatus similar in size to a Pitot Tube, but which would respond much more rapidly. One method which was considered, and which seemed to fulfil the requirements was to introduce air as an intermediate fluid between a U-tube manometer and the orifice of the measuring probe. The measuring probe was similar to a standard Pitot Tube, and was intended to read stagnation pressure only. At the outset, it was felt that some optical apparatus would be required with which to view the orifice of the probe. In this way, the air-water interface could be moved by small adjustment of the probe system pressure, and could therefore be aligned into some fixed reference position,

probably by means of cross-hairs on the optical apparatus. However, subsequent experimentation proved that an extremely stable situation seemed to present itself in that, when the air loop of the probe system had been pressurized, and the air allowed to escape from the probe tip in the form of bubbles, the emission of the bubbles from the probe terminated very abruptly, and a stable manometric head reading was observed. The foregoing observation was made with a probe which was simply immersed in a container of water to a known depth, with no fluid velocities present. This pressure head was higher than the hydrostatic pressure head by an amount which was due to the surface tension forces acting on the air-water interface present at the probe tip.

The fact that a stable reading would be observed in a probe which was being used for velocity measurment would also be expected. While the bubbles of air were breaking off the tip of the probe, a condition of unstable equilibrium would be present, in that the manometric head would be greater than the sum of the surface tension and stagnation heads.# When the manometric head became equal to the sum of the stagnation and surface tension heads, a condition of unstable equilibrium would prevail, and any slight disturbance would cause a further bubble to break off the probe tip. At this time, a condition of metastable equilibrium would prevail, and a combined head would be observed on the manometer which would be

---

In the context of this thesis, the term "stagnation pressure" is used to denote the sum of the hydrostatic and dynamic pressures.

less than the normal manometric head , the difference, however, being negligibly small. The combined head referred to is the sum of the velocity head, hydrostatic head and surface tension head. The velocity profiles measured with this probe are shown in figure 14.

Figure 16 shows a cross-sectional view of a type of Pitot-Static tube also designed to use the air-ejection principle. The overall dimension ratios are those recommended for the construction of standard Pitot-Static tubes (14). However, the probe is designed so that there are no sharp corners or unnecessary voids within the fluid lines of the probe where the water could become trapped and possibly give rise to erroneous pressure readings. Also, the static orifice had been counterbored so that the air-water interface which, through judicious selection of the counterboring dimensions, would attach itself to the periphery of the orifice at the base of the counterbore, would not present itself to the main body of the fluid, and thus would not affect the streamline pattern and the static pressure in its immediate vicinity. The stagnation orifice was similarly counterbored so that the two orifices, being similar, would not produce any unexpected measurement error due to the counterbore.

The plain stagnation head measuring air-ejecting probe was used instead of the Pitot-Static type in the experimental work reported in this thesis for the following reasons:

(i) The extra time required to operate two air-ejecting probe orifices rather than one would have increased the test time

to such an extent that the time dependence of the test fluid might have become significant.

(ii) The simple stagnation pressure measuring probe could be manufactured with greater ease and in smaller sizes than could the air-ejecting Pitot-Static probe.

(iii) The static pressure varied only with the fluid depth in this type of flow field, and therefore a static tube mounted on the main chamber will give the static pressure at the measuring point. (This fact has been previously alluded to in the text of this thesis, and reference made to justify its use in the footnote on page 14.)

In carrying out this part of the experimental work it was observed that each manometric head reading could be accomplished in about one minute and, as a result, the test run that was made with a 50 P.P.M. solution concentration of the polyacrylamide MRL-159 took less than ten minutes.

The shortness of the test time, as well as the fact that the circulating pump and the temperature control vessel agitator were not in operation throughout the test, and that the disk speed was considerably less than that used in previous parts of the experimental work (825 R.P.M. as compared with an average of 1268 R.P.M. for the drag reduction tests) meant that the degradation of the polymer by shear was minimized, and indeed could be disregarded. It certainly would contribute far less than the one half percent drag increase predicted for a full ten minutes of testing time by the curve for

MRL-159 in figure 12, in which the fluid was subjected to the shear of the circulating pump and the temperature control vessel agitator.

6. ANALYSIS OF EXPERIMENTAL RESULTS

In this chapter the form in which the results are derived from experimental procedure, and the form in which they are presented will be considered. The experimental values obtained from this analysis are presented in the Appendix, Section A.

As a preliminary to the main experiment, a test run for distilled water was undertaken from which it was required to plot a curve of Reynolds Number vs. Dimensionless Moment Coefficient. (The details of this preliminary run were described in section 4.1 entitled "Verification of Measuring Apparatus".) The Reynolds Numbers and Dimensionless Moment Coefficients were calculated from the following two expressions, which are true for fully immersed rotating disks:

$$R_n = \frac{R_{(e)}^2 \omega}{V}$$

$$C_m = \frac{2T_d}{\rho \omega^2 R_{(e)}^5}$$

Where: R_n is the Reynolds Number

$R_{(e)}$ is the expanded disk radius

ω is the disk speed

V is the dynamic viscosity

C_m is the Dimensionless Moment Coefficient

T_d is the torque due to drag of the disk #

These symbols are also defined in chapter 11, "Nomenclature".

ρ is the density of the fluid

All torque values were calculated from the dynamometer load values using the simple moment relationships:

$$T_o = A \times L_o \qquad T_d = A \times L - T_o$$

Where: T_o is the dynamometer torque due to bearing and seal friction

T_d is the torque due to hydrodynamic drag alone

A is the dynamometer moment arm

L_o is the dynamometer load due to bearing and seal friction

L is the gross dynamometer load for a given test condition

The first relationship evaluates the torque due to all mechanical losses in the equipment, with the exception of the static torque in the dynamometer mount bearings, which would be negligible. The second relationship evaluates the torque due to hydrodynamic drag alone.

Throughout all of the experimentation, the concentration values of the polymer solutions are reported. The solutions are divided into two categories: Stock Solutions and Test Solutions. The relationships used in determining the concentrations of the Stock and Test Solutions were simplified from the rigorous relationships as follows:

$$\text{True Concentration of Stock Solution, } C_s = \frac{Wd.p \times 10^6}{W_{w.s} + W_m}$$

Approximated Value of Stock Solution Concentration, $C_s \approx \frac{W_{d.p} \times 10^6}{W_{w.s}}$

Where: $W_{d.p}$ is the weight of the dried polymer

$W_{w.s}$ is the weight of water added to the polymer

W_m is the weight of moisture in the polymer sample

True Concentration of Test Solution, $C_t = \frac{W_{d.p} \times 10^6}{W_{w.t} + W_{w.s} + W_m}$

Approximate Concentration of Test Solution, $C_t \approx \frac{C_s}{1 + W_{w.t}/W_{s.t}}$

Where: $W_{w.t}$ is the weight of water added to form the test solution

$W_{s.t}$ is the weight of stock solution added to form the test solution

The maximum error incurred in using these approximations is 0.04%, and, being so insignificant, is not even mentioned in Chapter 7, entitled "Error Analysis".

6.1 Drag Reduction Test Results

The only relationships which were required in order to calculate the reduction in drag are the aforementioned relationship used to calculate the torque due to drag, and the following relationship which expresses the reduction in drag as a percentage:

Reduction in Drag, R.D. $= \frac{T_{d(\text{reference fluid})} - T_{d(\text{test fluid})}}{T_{d(\text{reference fluid})}} \times 100\%$

The reference fluid in all cases was distilled water.

6.1.1 Time Rate of Torque Variation, and Resultant Modification of Drag Reduction Results

It was the purpose of this phase of the experimental work to find some way of correcting the data obtained from the drag reduction tests so that allowance could be made for the variation of drag with time. This would make the results of the drag reduction tests independent of the shear characteristics of the apparatus, and hence any other unshrouded disk apparatus employing the same disk speed and disk radius would yield comparable results.

The time rate of torque variation was evaluated for 50 P.P.M. solutions of the polyacrylamides MRL-159 and MRL-295, and the results are portrayed in figure 12, as well as in tabular form in the Appendix, Section A. The increase in drag as a function of time was evaluated from this curve by considering all test readings to have been taken thirty minutes after start-up, thirty minutes being the time lapse between start-up and the mid point in time of the testing period in the drag reduction evaluation tests.

This approximation is justifiable because the rate of change of drag is seen to be roughly linear in the testing time region around the thirty minute position.

Since the increase in drag is a result of the polymer molecules shearing, and since, in very weak solutions the proportion of polymer molecules which underwent rupture shear would be a function of their concentration, the increase in drag due to shear can be calculated for solution concentrations other than 50 P.P.M. by direct proportion in terms of concentration. For example, a five

P.P.M. solution concentration could be expected to suffer only one tenth of the drag increase of the 50 P.P.M. solution when both were tested under similar test conditions.

The Increase in Drag is evaluated from the following relationship:

$$I.D. = \frac{T_{d(n)} - T_{d(o)}}{T_{d(o)}} \times 100\%$$

Where: $T_{d(n)}$ is the torque due to drag at an elapsed time of n minutes

$T_{d(o)}$ is the torque due to drag at the beginning of the test

Using this analysis, curves of drag reduction vs. concentration of polymer effectively extrapolated to zero time were obtained for the polyacrylamides MRL-159 and MRL-295, and are presented in figure 13.

6.2 Velocity Profile Results

In the evaluation of the tangential velocity readings at different points within the boundary layer of the disk, the following relationships were used:

$$V_f = \sqrt{2gh}$$

$$h = H - h_s - h_{st}$$

$$h_{st} = \frac{2T_{st}}{\gamma_w \times R_p}$$

Where: V_f is the velocity at the measuring point

g is the acceleration due to gravity

h is the velocity head

H is the manometric head

h_s is the hydrostatic head

h_{st} is the surface tension head

T_{st} is the air water interface surface tension (8)

γ_w is the specific weight of the water

R_p is the inside radius of the probe

The velocities thus obtained were then rendered dimensionless by dividing each velocity relative to the disk in turn by the velocity relative to the disk at the outside edge of the boundary layer. In a similar way the distances from the face of the disk to each point of velocity measurement were then rendered dimensionless by dividing them by the total boundary layer thickness.

The corresponding dimensionless velocities and displacements were then plotted in figure 14 to show the shape of the velocity profiles in the boundary layer for water, and that for a 50 P.P.M. solution of the polyacrylamide MRL-159.

7. ERROR ANALYSIS

The purpose of this chapter is to provide a comprehensive list of the error content of the experimental work inasmuch as it affects the results thereof. Discussion of some quantities for which the strict mathematical error does not fully occur in practice, or for which that error is somewhat misleading is also undertaken here.

Errors which are insignificantly small are not even calculated here, as to do so would be an academic exercise and would not contribute to the utility of the error analysis. However, their magnitude may be briefly alluded to elsewhere in the text.

7.1 Presentation of Experimental Errors

In this section the maximum error, being the sum of the maximum instrument error and the maximum experimental error is based partly upon manufacturers' data, and partly upon the judgement of the author. Some of the errors which occur in practice are extremely difficult to evaluate. In particular, those errors concerned with the velocity profile measurement in the boundary layer are difficult to evaluate. For those measurements, the errors stated must be considered to be qualified estimations only. However, since the velocity profiles are only qualitatively employed to support one theory on the drag reduction mechanism, the errors are not of extreme consequence.

DESCRIPTION	SYMBOL	INSTRUMENTAL ERROR	EXPERIMENTAL ERROR	MAXIMUM ERROR
Sample Moisture Content	W_m	Negligible	±2%, due to atmospheric contact after oven drying, before re-weighing	±2%
Disk Speed	ω	±1%	±1%, due to coarseness of the scale	±2%
Dynamometer Load	L	±1%	±1% due to small vibrations of the scale needle	±2%
Velocity Probe Position	x	±3%	±3%, due to uncertainty in exact start position of the probe	±6%
Manometric Head	H	±2%	+0% -3%, due to the possibility of turbulent release of some bubbles	+2% -5%
Temperature of Test Fluid	t	±2% (±1F°)	±2%, due to small thermal gradients	±4%
Kinematic Viscosity	V	Determined from tables (9) as a function of fluid temperature	±4%, due to approximately 1:1 ratio of V to t (9)	±4%
Velocity Probe Measuring Radius	R_m	±1%, ±1/32 of an inch, using steel scale	±1%, due to flexibility of the probe	±2%
Dynamometer Moment Arm	A	±1%, ±1/32 of an inch, using steel scale	±2%, due to difficulty in discerning true end points of the arm	±3%

DESCRIPTION	SYMBOL	INSTRUMENTAL ERROR	EXPERIMENTAL ERROR	MAXIMUM ERROR
Disk Radius	R	±0.2%, measured with vernier caliper	±0.2%, reading error on vernier caliper	±0.4%
Inside Bore of Probe	R_p	±5%, Manufacturer's specifications for hypodermic tubing	-0-	±5%
Air-Water Interface Surface Tension	T_{st}	±2%, assumed from presentation of values	-0-	±2%
Hydrostatic Head	h_s	-0-	±2% reading error	±2%

DESCRIPTION	SYMBOL	RELATION	MAXIMUM UNCERTAINTY
Reynolds Number	R_n	$R_n = \frac{R^2 \omega}{V}$	± 12%
Bearing and Seal Friction Torque	T_o	$T_o = A \times L_o$	± 5%
Gross Torque	T	$T = A \times L$	± 5%
Net Torque	T_d	$T_d = A \times L - A \times L_o$	± 5%
Dimensionless Moment Coefficient	C_m	$C_m = \frac{2T_d}{\rho \omega^2 R^5}$	± 11%
Stock Solution Concentration	C_s	$C_s = \frac{W_{d.p} \times 10^6}{W_{w.s}}$	Error Negligible
Test Solution Concentration	C_t	$C_t = \frac{C_s}{1 + W_{w.t}/W_{s.t}}$	Error Negligible
Reduction in Drag	R.D.	$R.D. = \frac{T_{d(\text{reference fluid})} - T_{d(\text{test fluid})}}{T_{d(\text{reference fluid})}}$	±10% (± 2.5%)#
Increase in Drag	I.D.	$I.D. = \frac{T_{d(n)} - T_{d(o)}}{T_{d(o)}}$	±10%

Maximum Uncertainty Ranges in parentheses denote probable maximum uncertainties, and are more meaningful. Refer to pages 43 and 44 for their assessment.

DESCRIPTION	SYMBOL	RELATION	MAXIMUM UNCERTAINTY
Surface Tension Head	$h_{s.t}$	$h_{s.t} = \frac{2T}{\gamma_w x R_p}$	±7%
Velocity Head	h	$h = H - h_s - h_{s.t}$	±11%
Velocity of Fluid	V_f	$V_f = \sqrt{2gh}$	±5.5% (±15%)#

Maximum Uncertainty Ranges in parentheses denote probable maximum uncertainties, and are more meaningful. Refer to pages 43 and 44 for their assessment.

7.2 Further Discussion of Errors

Although the maximum uncertainty stated in the foregoing table for the reduction in drag is 10%, this value, derived from simple mathematical relationships, is not representative of the probable maximum error which would be expected. This is so because the error is not categorically discriminated in the calculation. In effect, any systematic, or biased errors which might occur in evaluating the torque due to drag would almost certainly occur in both test and reference fluids in the same magnitude, and so would not affect the drag reduction value. This error would be the result of a zeroing error in either the speed or the dynamometer load readings, or incorrect evaluation of the dynamometer moment arm. Furthermore, since all torque values were averaged from four readings, the maximum probable error to be expected would be one quarter of that which would be likely to occur in a single reading. It would therefore have a value of 2.5%.

As a result, it would be more proper to evaluate the excellence of the quantities connected therewith using the maximum probable error rather than the maximum possible error (or maximum uncertainty) as a criterion.

This consideration would yield the following:

Description	Symbol	Maximum Probable Error
Gross Torque	T	$\pm 1.25\%$
Net Torque	T_d	$\pm 1.25\%$
Reduction in Drag	R.D.	$\pm 2.5\%$

It is also necessary to explain that the maximum uncertainty listed for the boundary layer velocity values of ± 5.5% does not properly signify the accuracy of the experimental values, or of the velocity profiles shown in figure 12. Although it is true to say that the measured velocity has associated with it a maximum uncertainty of ±5.5%, it is also necessary to realize that a given velocity value has associated with it a certain position within the boundary layer, and that this position also carries with it an uncertainty. Therefore, assigning a given velocity to a given position would have a maximum uncertainty of at least the sum of the maximum uncertainties associated with velocity and position, namely, ± 11.5%. The maximum uncertainty of the velocity at a given position was even higher due to the fact that the velocity gradient would be a non-linear function of the distance from the disk, and the assumption that the average velocity vector across the probe occurred at the geometric centre of the orifice would carry some inaccuracy.

This latter inaccuracy is usually ignored as being insignificant; however in this case, the dimensions of the probe tip are not insignificantly small when compared with the dimensions of the boundary layers encountered. As a result, the maximum uncertainty which can be associated with a velocity vector assigned to a given distance from the disk face would probably be about ±15%.

8. DISCUSSION OF RESULTS

It is difficult to compare the results of the experimental work with previous research. Only two previous studies on the effect of dilute aqueous polymer solutions on the hydrodynamic drag were found in which the concentration range was similar to that of this experimental work (1,5). However, neither of these reports contained sufficient detail in their procedures and results to permit any worthwhile comparison of a quantitative nature.

Hamill (5) reported some details of the test solution preparation procedure used by him. Neither Hamill (5) nor Hoyt and Fabula (1) reported making allowance for the sample moisture content, time rate of increase of drag, or hardness of the water used by them as a test solvent.# They did not report test procedure, test solution temperature, or the formula designation of the guar gum used. Comparison of figures six and seven show that different types of guar gum do indeed exhibit varying drag reduction qualities. Neither report shows the experimental data points on their curve of drag reduction vs. concentration, indeed, it is conjectured that the curve portrayed in the report of Hoyt and Fabula, being shown as a straight line, might have been produced from only one or two experimental observations.

In a discussion with him, Hamill revealed that these three factors were indeed not taken into consideration by him in his study.

8.1 Drag Reduction Test Results

The drag reduction vs. concentration curves obtained for the five polymers tested and portrayed in figures 6 to 11 inclusive were, for the most part, what was expected. However, since previous work by Hoyt and Fabula, and by Hamill showed guar gum to be the most effective additive, then it is significant to have accumulated considerable data for the polyacrylamides MRL-159 and MRL-295, which were found to have far greater drag reduction qualities in aqueous solution than guar gum. The provision for the extrapolation of the drag reduction results to zero test time leads to the possibility of correlation between this work, and that which may be conducted in the future, provided either that the disk size and speed are the same, or that some relationship be developed to relate disk size and speed to relative drag reduction. These zero time results might also be of interest in ship model testing where a negligible time increase of drag would be expected as a result of shear. Furthermore, in the field of model testing, the drag reduction effect may provide an additional variable in the application of dimensional analysis.

In all the experimental results of drag reduction vs. concentration, with the exception of the low concentration portion of the relation for guar gum A-20-D, an increase of disk speed for a given concentration resulted in an increase of the drag reduction. Bearing in mind that Toms (3) discovered that small concentrations of polymers had no effect on the hydrostatic drag in the laminar

flow regime of a solvent, and that successive increases in speed expand the turbulent flow regime on the rotating disk by successively smaller increments, it can be concluded, both from the difference in the effect of speed on the drag reduction vs. concentration curves for different substances, and from the fact that additional increments of speed in most of the tabular results (Appendix, Section A) do not cause successively diminished increases in drag reduction; that the variation in speed causes changes in the velocity profiles, and hence in the drag reduction characteristics within the turbulent boundary layer.

A levelling off of the drag reduction caused by increased concentrations of all polymers tested would indicate that the drag reduction property of the polymers will reach a saturation point which is a function of the concentration. Indeed, the polyacrylamides MRL-159 and MRL-295 may reach this point in the 100 to 200 P.P.M. concentration range. At this concentration even the most precise viscosimeter (operating in the laminar regime) fails to report any significant change in the viscosity as compared to that for water.

Considering further that the hydrodynamic drag in the laminar flow regime has remained unaffected, it may be stated that the observed phenomena are not merely the normal tendencies of a power law fluid of the pseudoplastic variety. (A pseudoplastic power law fluid is represented by the stress strain relation $\tau = \mu \left(\frac{du}{dx}\right)^n$ where the index 'n' is positive, and has a value of less than unity.)

The evaluation of the drag increase as a function of the time that a fluid is subjected to shear was only undertaken for the polyacrylamides MRL-159 and MRL-295 for two reasons:

(i) These two polyacrylamides were the most effective drag reduction agents, and were the only ones subjected to further analysis for this reason.

(ii) None of the other polymers was observed to cause significant differences in dynamometer load for a given disk speed with successive readings which were taken at about minute intervals. Consequently, unless they were used in a situation where they were subjected to intense and prolonged shear, their behavior could be considered to be non-rheopectic (non time dependent).

That these two polyacrylamides exhibited almost identical drag reduction vs. concentration relations when extrapolated to zero time is probably coincidental. The polyacrylamide MRL-19 would not have done so, but would have been far below these two in drag reduction effectiveness. It is interesting to note that the stock solution of MRL-295 at a concentration of 2,000 P.P.M. was visibly more viscous than that of MRL-159 at a concentration of 4,000 P.P.M., further supporting the supposition that there is no direct relation between viscosity and drag reduction characteristics at low polymer concentrations.

8.2 Theories on Drag Reduction

Three general theories have been put forth to explain the observed drag reduction phenomenon which occurs with the addition of trace quantities of certain polymers to solvents. These three theories cannot be attributed directly to any particular investigator; rather, they just appear as conjectures in some of the literature studied. The three theories are as follows:

Transition Offset Theory

In any flow pattern taking place in a fluid to which has been added certain polymers in trace quantities, the transition regime is offset so that it occurs at abnormally high Reynolds Numbers, that is, Reynolds Numbers in excess of 2,000 for pipe flow, and in excess of 3×10^5 for flow near a rotating plane. Otherwise, the nature of the laminar and turbulent flow regimes would remain unaffected.

Standard Pseudoplastic Theory

In any flow pattern taking place in a fluid to which has been added certain polymers in trace quantities, the fluid will become inherently pseudoplastic, having previously been Newtonian, and its stress-strain relation will be given by $\tau = V\left(\frac{du}{dx}\right)^n$, $0 < n < 1$. The apparent viscosity V decreases with increasing shear rate.

Turbulent Suppression Theory

In any flow pattern taking place in a fluid to which has been added certain polymers in trace quantities, the flow characteristics of the fluid will be unchanged in the laminar flow regime, but the eddies occurring in the turbulent flow regime will tend to be suppressed. The flow in the turbulent regime will therefore tend to dissipate less energy than was the case before the addition of the polymers.

8.3 Evaluation of the Theories Using Boundary Layer Velocity Profile Results

As has been stated earlier in this thesis, the boundary layer velocity profiles as such are probably not precise enough to be used in any quantitative manner. However, it can be readily seen that the velocity profile in the boundary layer of the MRL-159 solution is considerably less turbulent than that of plain water.

It is possible to calculate a "Hypothetical Transition Reynolds Number" or a "Hypothetical Transition Radius" which would, assuming the transition offset theory to be applicable, be a direct function of the drag reduction. In this context, calculations were made with some of the data of the velocity profile measurement tests in which the observed drag reduction was approximately 30%. (actually 29.8%)

Using an iterative procedure, a transition radius was determined at which turbulence would commence. This hypothetical transition

radius would be of such a value that, using hydrodynamic drag relations for the laminar and turbulent flow about a rotating disk, a drag reduction of 30% would occur due to transition offset, with respect to distilled water as the datum fluid. The determination of this hypothetical transition radius is presented in the Appendix, Section D, and the value calculated was 5.1 inches.

The transition offset theory would thus predict that at radii on the disk in excess of 5.1 inches, fully turbulent flow would be expected and, as this is contrary to the observations for the polyacrylamide MRL-159, the transition offset theory is rejected as a total explanation of the drag reduction phenomenon. Furthermore, Dodge and Metzner (10) show experimentally that, in pipe flow, the transition Reynolds Number was 3100 for a polymer concentration in excess of 11.8%. The Reynolds Number under our experimental conditions at a radius of 5.1 inches was 1.58×10^6. To further relate these two sources of data we can say that we would have to expect a solution concentration of 0.005% to increase the transition Reynolds Number by a factor of five; whereas previous experimentation shows a transition Reynolds Number increase of only 1.5 for a solution concentration in excess of or equal to 11.8%

It is concluded therefrom that the "Transition Offset Theory" is incorrect, except in that it may account for a very slight and probably immeasurably small increase in the transition Reynolds Number, and hence an immeasurably small decrease in the hydrodynamic drag.

Two factors support the rejection of the "Standard Pseudoplastic Theory". Firstly, it has already been substantiated that the laminar flow phase of low concentration solutions of long chain polymers is not any different than that of the pure solvent in which they are dissolved. Secondly, the average values of the power law index for the drag reducing polymer "Carbopol" has been plotted as a function of concentration, data points being extracted from reference 10, and the data point for zero concentration being unity by definition (figure 17). Although the extrapolation is rather coarse, it is very evident that the power law index at concentrations of less than 100 P.P.M. for a drag reducing polymer dissolved in water is extremely close to unity. As a consequence, the fluid is, for all practical purposes, Newtonian.

The first factor mentioned above would tend to indicate that the test solutions being investigated are non-pseudoplastic. The second factor indicates that, even if these solutions were pseudoplastic, the degree of pseudoplasticity, as characterised by the power law index, would be negligible.

Contrary to the latter two, the "Turbulent Suppression Theory" does not appear to be in conflict with the results presented in any of the literature. Furthermore, it is in accordance with the general shapes of the velocity profiles in the boundary layer as presented in figure 14. If the turbulent eddies tended to be suppressed in a direction orthogonal to the disk face with the addition of drag reducing polymers to a solvent, the rate of energy

dissipation by turbulence would be reduced, and the boundary layer would become more nearly laminar in nature (where the nature of the boundary layer is characterised in part by its velocity profile). Also, in accordance with the observed results, the turbulent boundary layer would not be expected to propagate out towards the free stream to such an extent as would be the case for the pure solvent. We would expect a thinner boundary layer, and this also is in accordance with the observations made during the experimental work.

8.4 Phenomenological Model of the Turbulent Suppression Theory

Without concerning ourselves with molecular mechanics to any great extent, it is possible to present a model which might explain the observed phenomenon of drag reduction in dilute polymer solutions. As these polymer molecules are random-coiled and non-associating, and also as their bonding energy is relatively low, they can be expected to undergo "mechanical" changes when subjected to shear.

Consider a molecule which may be made up of many thousands of molecular units, or mers forming a straight chain configuration; and which, under zero shear conditions is approximately spherical in its random coiled form. If this molecule is placed in the velocity gradient associated with a boundary layer, then the shear stresses applied to the molecule could cause it to elongate into approximate alignment with the flow direction. A dilute solution of these polymers would, in effect, tend to contain "molecular curtains" of these elongated molecules in areas of high velocity gradients, namely, in boundary layer regions.

These "molecular curtains" would tend to suppress the turbulent eddies from propagating out from the boundary in a direction orthogonal to it, and hence orthogonal to the direction of elongation of the molecules. By this mechanism the turbulent dissipation of energy would decrease, and the boundary layer velocity profile would be altered and could be expected to look more nearly laminar. The "molecular curtains" would not impede the overall fluid flow.

Although this model may not have much importance in terms of the engineering significance of these drag reducing polymers, it could be used to explain all phenomena which have been observed to date. Dodge and Metzner (10) have observed that the turbulent eddies are suppressed in a direction orthogonal to the flow in solutions of high polymer concentration (considerably higher than used in this research) ranging from 0.2% to 15% by weight. They attribute this to a positive pseudoplastic viscosity gradient in the outer regions of the boundary layer, moving outwards from the boundary. However, since this phenomenon appears to be present also in solutions of minute polymer concentration, there must be an explanation thereof which does not depend on a viscosity gradient , and the model set forth here to explain the suppression of turbulence would fit the requirements.

9. RECOMMENDATIONS

In assessing the experimental work to date, it would seem that there are three general areas of information which have remained undeveloped as yet.

The first area is directly connected with the commercial utilization of drag reducing chemicals, and especially to those which are water soluble. It would be very useful to develop a set of drag reduction vs. concentration characteristics, and perhaps also a set of shear duration vs. shear degradation characteristics for the more effective polymers investigated in this thesis, for pipe flow. The same concentration range should be investigated. Having these two sets of characteristics as well as those presented in this thesis, first approximations could be made of the possible head loss recovery in a pumping system containing rotary pumps.

The second area would be concerned with the design of a small, relatively inexpensive and yet accurate rotating disk apparatus which could be used to obtain a direct reading of the characteristic drag reduction of the water in model testing basins. It would involve much original design work, and then calibration against drag reduction as measured, for example, on a standard ship testing model.

The third area in which investigation would be useful is the further study of the boundary layers which occur in solutions of drag reducing polymers. These could be investigated with respect to turbulence measurement and evaluation of universal velocity

distributions, both related to the solution concentration, and hence to the effective drag reduction capabilities of the solution. This investigation would also probably require a pipe flow configuration, and visual methods could be used to study the turbulence. (3,10,15) Dye injection techniques have been used to propose theories on the mechanism of drag reduction (10). However, section 8.4 of this thesis suggests that the theories concluded therefrom were probably not correct, at least inasmuch as very dilute polymer solutions are concerned.

Reference 16 is concerned with a photographic technique involving the timed release of gas bubbles by electrolysis from a fine wire within the boundary layer. These releases are synchronized with a motion picture camera, and have been successfully applied to velocity measurements in thin aqueous boundary layers. However, great pains would have to be taken to ensure that the bubble streaks were fine enough to make possible the visualization of turbulent eddies.

From such a study it might be possible to construct relations which would permit the calculation of the drag reduction for different polymers.

10. CONCLUSIONS

The design of a rotating disk apparatus which is sufficiently sensitive in drag measurement, and in which the disk is hydrodynamically unshrouded has led to a series of curves of drag reduction vs. concentration for aqueous solutions of certain long chain polymers. These curves are more precise than those contained in previous literature for concentrations below 100 P.P.M. Allowance for polymer sample moisture content and for time rate of drag variation (rheopecticity), as well as very careful preparation, storage and evaluation techniques have added to the accuracy as well as to the precision of these curves.

A new type of velocity measuring probe and ancillary equipment connected therewith has been developed to make possible velocity head evaluation with rapid response, as well as with a small probe orifice. Measurement of a set of boundary layer velocity profiles for a 50 P.P.M. solution concentration of the polymer MRL-159 has provided an insight into the mechanism by which drag reducing polymers affect the dynamics of a solvent.

These profiles have made it possible to decide which theory for the reduction in hydrodynamic drag best explains the observed phenomena. From this decision, a phenomenological model has been postulated which would explain the mechanism of drag reduction, and which would be in accordance with the observations of previous investigators.

11. NOMENCLATURE

Symbol	Description	Units
A	Dynamometer Moment Arm	Ft.
C_s	Stock Solution Concentration (by weight)	Parts per Million (P.P.M.)
C_t	Test Solution Concentration (by weight)	Parts per Million (P.P.M.)
g	Acceleration Due to Gravity	Ft./Sec.^{2}
H	Manometric Head	Ft.
h	Velocity Head	Ft.
h_s	Hydrostatic Head	Ft.
h_{st}	Surface Tension Head	Ft.
$L_.$	Dynamometer Gross Load	Lbs.$_f$
L_o	Dynamometer Load Due to Frictional Losses	Lbs.$_f$
R	Disk Radius	Ft.
R_m	Radius from Disk Centre to Probe Measuring Point	Ft.

Symbol	Description	Units
R_p	Inside Radius of Probe Orifice	Ft.
t	Temperature of Test Fluid	^oF
T_o	Dynamometer Torque Due to Frictional Losses	$Ft.-Lbs._f$
T_d	Dynamometer Net Torque (Torque Due to Drag)	$Ft.-Lbs._f$
T_{st}	Interface Surface Tension	$Lbs._f/Ft.$
u	Local Velocity Vector	Ft./Sec.
V	Kinematic Viscosity	$Ft.^2/Sec.$
V_f	Fluid Velocity (at points within the boundary layer)	Ft./Sec.
$W_{d.p}$	Weight of Dry Polymer	$Lbs._m$
W_m	Weight of Moisture in Polymer Sample	$Lbs._m$
$W_{s.t}$	Weight of Stock Solution Added to the Test Solvent	$Lbs._m$
$W_{w.s}$	Weight of Water Added to Form the Stock Solution	$Lbs._m$
$W_{w.t}$	Weight of Water Added to Form the Test Solution	$Lbs._m$
x	Distance Measured out from Face of Rotating Disk	Ft.

Greek Symbol	Description	Units
γ_w	Specific Weight of Test Fluid	$Lbs._f/Ft.^3$
δ	Boundary Layer Thickness	Ft.
μ	Dynamic Viscosity	$Lbs._f\text{-}Sec./Ft.^2$
τ	Shearing Stress of Test Fluid	$Lbs._f/Ft.^2$
ω	Disk Speed	R.P.M., (Rad/Sec.)
ρ	Density of Test Fluid	$Slugs/Ft.^3$

Dimensionless Parameters	Description
I.D.	Increase in Drag of Test Fluid
R.D.	Reduction in Drag of Test Fluid
R_n	Reynolds Number ($R_n = R_{(e)}^2 \omega/V$)
C_m	Dimensionless Moment Coefficient ($C_m = T_d/\frac{1}{2}\rho\omega^2 R^5$)
n	Power Law Index of Shear Equation ($\tau = V(du/dx)^n$)

12. REFERENCES

1. Hoyt, J.W. and Fabula, A.G., "Frictional Resistance in Towing Tanks", 10th. International Towing Tank Conference, (I.T.T.C.), London, Sept. 1963.

2. Ibid. p.4

3. Toms, B.A., "Some Observations on the Flow of Linear Polymer Solutions Through Straight Tubes at Large Reynolds Numbers", Proceedings of the International Rheological Congress, Scheveningen, Holland, 1948, p. II-135.

4. Shaver, R.G. and Merrill, E.W., "Turbulent Flow of Pseudoplastic Polymer Solutions in Straight Cylindrical Tubes", A.I.Ch.E. Journal, Vol. 5, No. 2, p. 181, June 1959.

5. Hamill, P.A., "A Preliminary Experiment on the Effect of Additives on Hydrodynamic Drag", National Research Council, Ship Section, Laboratory Memorandum No. MTB-65, Ottawa, 1964.

6. Merrill, E.W., Mickley, H.S., Ram, A. and Stockmayer, W.H., "The Second Newtonian Viscosity Number", Journal of Polymer Science, Part A, Vol. 1, pp. 1201-1213, 1963.

7. Simha, R. and Zakin, J.L., "Compression of Flexible Chain Molecules in Solution", The Journal of Chemical Physics, Vol. 33, No. 6, p. 1791, Dec. 1960.

8. Kaufmann, W., "Fluid Mechanics", McGraw-Hill Book Co. Inc., Toronto, 1963.

9. Schlichting, H., "Boundary Layer Theory", McGraw-Hill Book Co. Inc., Toronto, 1960.

10. Dodge, D.W. and Metzner, A.B., "Turbulent Flow of Non-Newtonian Systems", A.L.Ch.E. Journal, Vol. 5, p. 189, 1959.

11. Whistler, R.L. and Be Miller, J.N., "Industrial Gums", Academic Press, New York, N.Y., 1959.

12. Albertson, M.L., Barton, J.R. and Simons, D.B., "Fluid Mechanics for Engineers", Prentice-Hall Inc., Englewood Cliffs, New Jersey, April, 1961.

13. Ibid, Preface, Table III, p. III.

14. Prandtl, L. and Tietjens, O.G., "Applied Hydro and Aero Mechanics", Dover Publications Inc., New York, N.Y., 1957.

15. Lukasik, S., "Velocity Measurements in Thin Boundary Layers", Stevens Institute of Technology, Technical Memorandum, Hoboken, New Jersey, 1959.

16. Daily, J.W. and Nece, R.W., "Chamber Dimension Effects on Induced Flow and Frictional Resistance of Enclosed Rotating Disks", Transactions A.S.M.E., D-82, p. 217, 1960.

13. BIBLIOGRAPHY

Albertson, M.L., Barton, J.R. and Simons, D.B., "Fluid Mechanics for Engineers", Prentice-Hall Inc., Englewood Cliffs, New Jersey, April, 1961.

Clauser, F.H., "The Turbulent Boundary Layer", Advances in Applied Mechanics, Vol. 4, Academic Press, New York, N.Y., 1956.

Comolli, C.R., Keathley, W.C. and Due, H.F., "A Study of Pressure Prediction Methods for Low-Flow Radial Bladed and Unbladed Disks", Pratt and Whitney Aircraft, Florida Research and Development Center, Paper No. PWA FR-1296, Feb. 1965.

Daily, J.W. and Bugliarello, G., "Basic Data for Dilute Fiber Suspensions in Uniform Flow with Shear", Technical Association of the Pulp and Paper Industry (TAPPI), Vol. 44 (1961), pp. 497-512.

Daily, J.W. and Nece, R.W., "Chamber Dimension Effects on Induced Flow and Frictional Resistance of Enclosed Rotating Disks", Transactions A.S.M.E., D-82, p. 217, 1960.

Dodge, D.W. and Metzner, A.B., "Turbulent Flow of Non-Newtonian Systems", A.I.Ch.E. Journal, Vol. 5, 1959.

Due, H.F., "An Empirical Method for Calculating Radial Pressure Distribution on Rotating Disks", A.S.M.E. paper no. 65-WA/FL-10.

Granville, P.S., "The Frictional Resistance and the Boundary Layer of Flat Plates in Non-Newtonian Fluids", David Taylor Model Basin (D.T.M.B.) report no. 1579, Dec. 1962.

Hamill, P.A., "A Preliminary Experiment on the Effect of Additives on Hydrodynamic Drag", National Research Council, Ship Section, Laboratory Memorandum No. MTB-65, Ottawa, 1964.

Hoyt, J.W. and Fabula, A.G., "Frictional Resistance in Towing Tanks", 10th. International Towing Tank Conference (I.T.T.C.), London, Sept. 1963.

Kaufmann, W., "Fluid Mechanics", McGraw-Hill Book Co. Inc., Toronto, 1963.

Lukasik, S., "Velocity Measurements in Thin Boundary Layers", Stevens Institute of Technology, Technical Memorandum, Hoboken, New Jersey, 1959.

Merrill, E.W., Mickley, H.S., Ram. A.,and Stockmayer, W.H., "The Second Newtonian Viscosity Number", Journal of Polymer Science, Part A, Vol. 1, pp. 1201-1213, 1963.

Prandtl, L., "Essentials of Fluid Dynamics", Hafner Publishing Company, New York, N.Y., 1952.

Prandtl, L. and Tietjens, O.G., "Applied Hydro and Aero Mechanics", Dover Publications Inc., New York, N.Y., 1957.

Shaver, R.G. and Merrill, E.W., "Turbulent Flow of Pseudoplastic Polymer Solutions in Straight Cylindrical Tubes", A.I.Ch.E. Journal, Vol. 5, No. 2, June 1959.

Simha, R. and Zakin, J.L., "Compression of Flexible Chain Molecules in Solution", The Journal of Chemical Physics, Vol. 33, No. 6, Dec. 1960.

Schlichting, H., "Boundary Layer Theory", McGraw-Hill Book Co. Inc., Toronto, 1960.

Toms, B.A., "Some Observations on the Flow of Linear Polymer Solutions Through Straight Tubes at Large Reynolds Numbers", Proceedings of the International Rheological Congress, Scheveningen, Holland, 1948.

Wells, C.S. Jr., "Similar Solutions of the Boundary Layer Equations for Purely Viscous Non-Newtonian Fluids", National Aeronautics and Space Administration, Washington, D.C., Technical Note D-2262, Contract No. NASw-729, April, 1964.

Whistler, R.L. and Be Miller, J.N., "Industrial Gums", Academic Press, New York, N.Y., 1959.

Commercial Pamphlets:

"Hercules Cellulose Gum, Properties and Uses", Hercules Powder Co., Wilmington, Delaware, Form No. 862 10M 6-63 5552.

"Jaguar (R.T.M.) Guar Gum by Stein Hall", Stein Hall and Co. Inc., New York, N.Y., 1962.

"Methods of Preparation and Use for Stein Hall Products in the Mining, Metallurgical, and Water Treatment Industries", Stein Hall and Co. Inc., New York, N.Y.

14. ILLUSTRATIONS

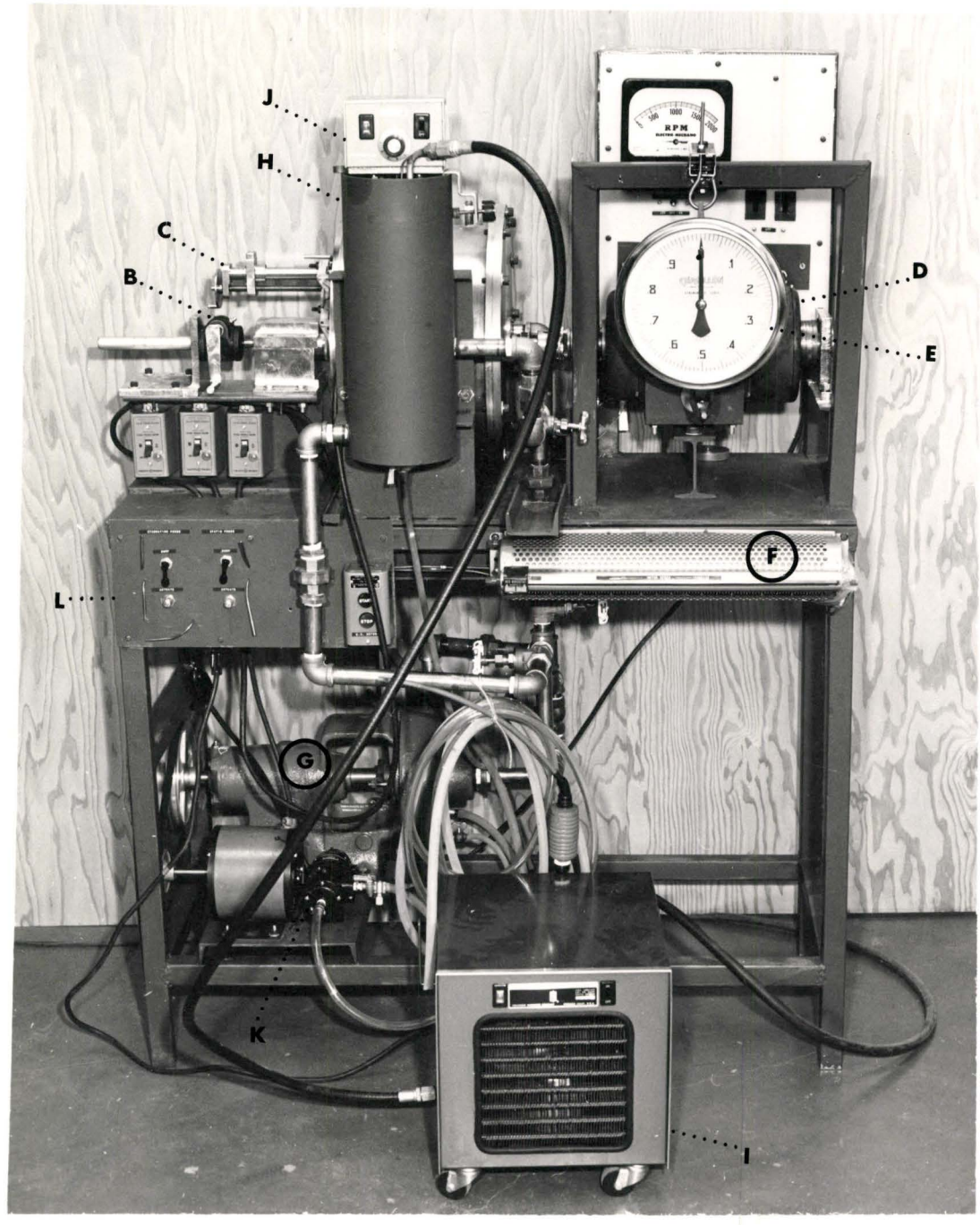

Figure 1A. The Main Testing Facility. Capital letters refer to the text, sections 3.1.1 to 3.1.6.

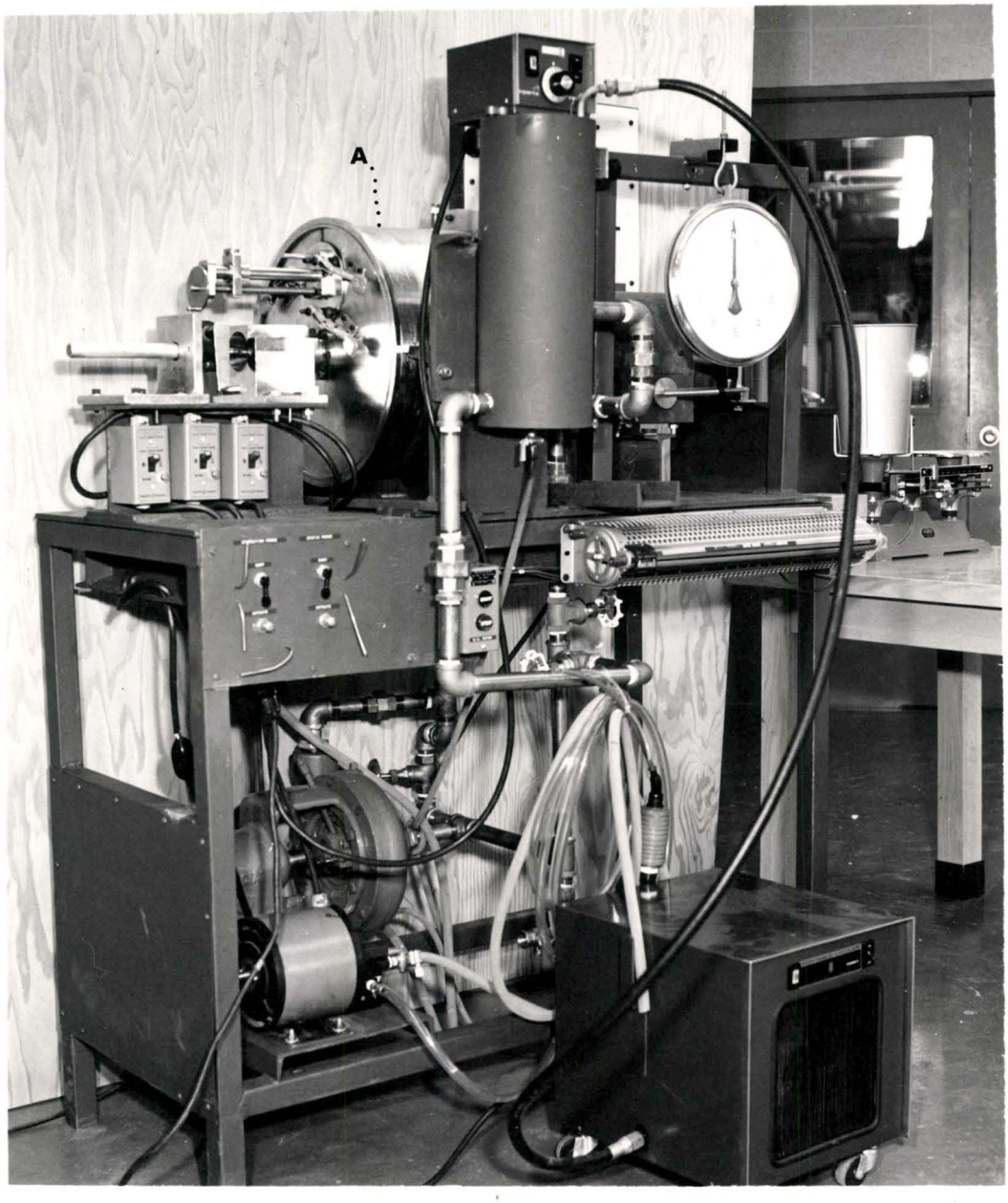

Figure 1B. The Main Testing Facility. Capital letters refer to the text, sections 3.1.1 to 3.1.6.

Figure 2. Holding Drums, in which test solutions were stored and agitated.

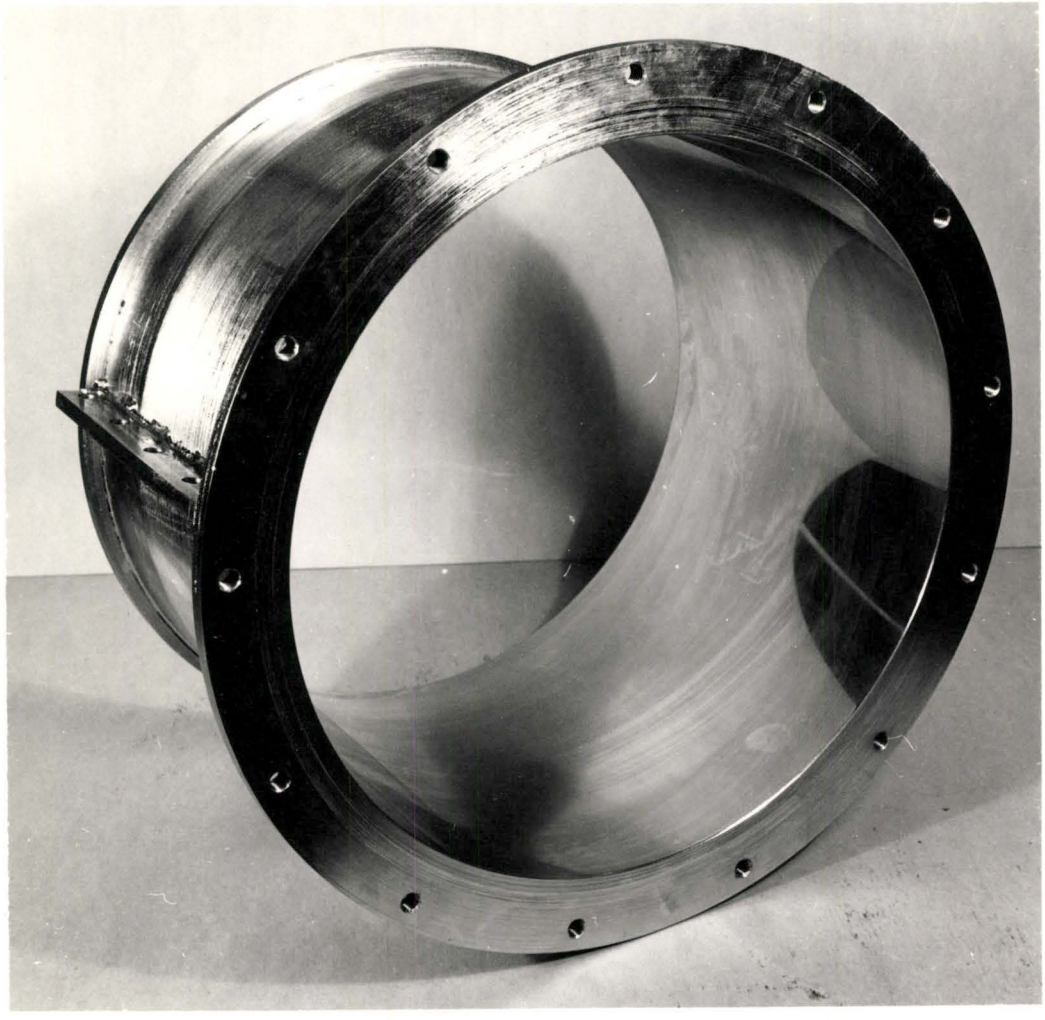

Figure 3. Major Section of the Main Chamber, showing microhoned interior surface.

PNEUMATIC AND HYDRAULIC SCHEMATICS

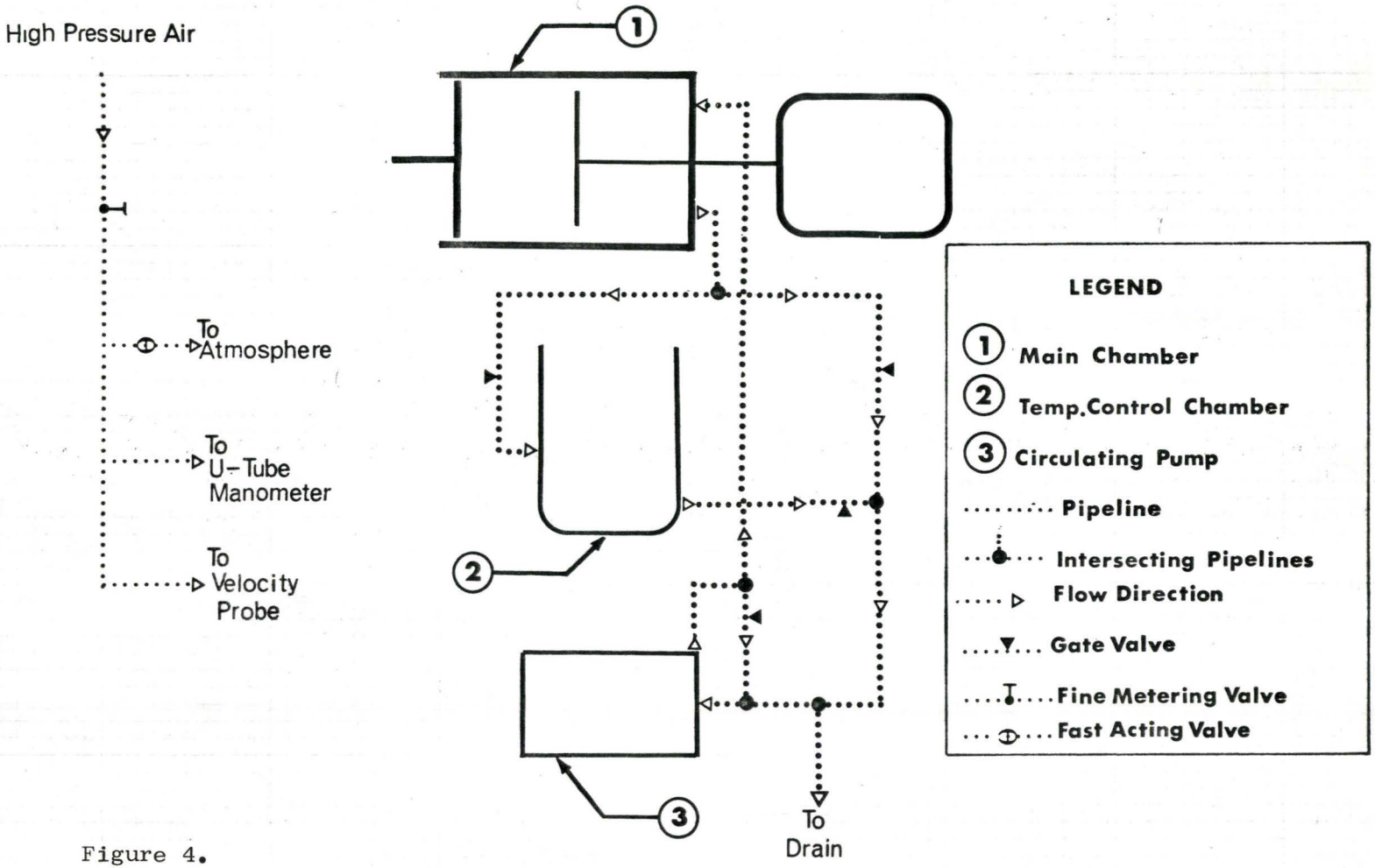

Figure 4.

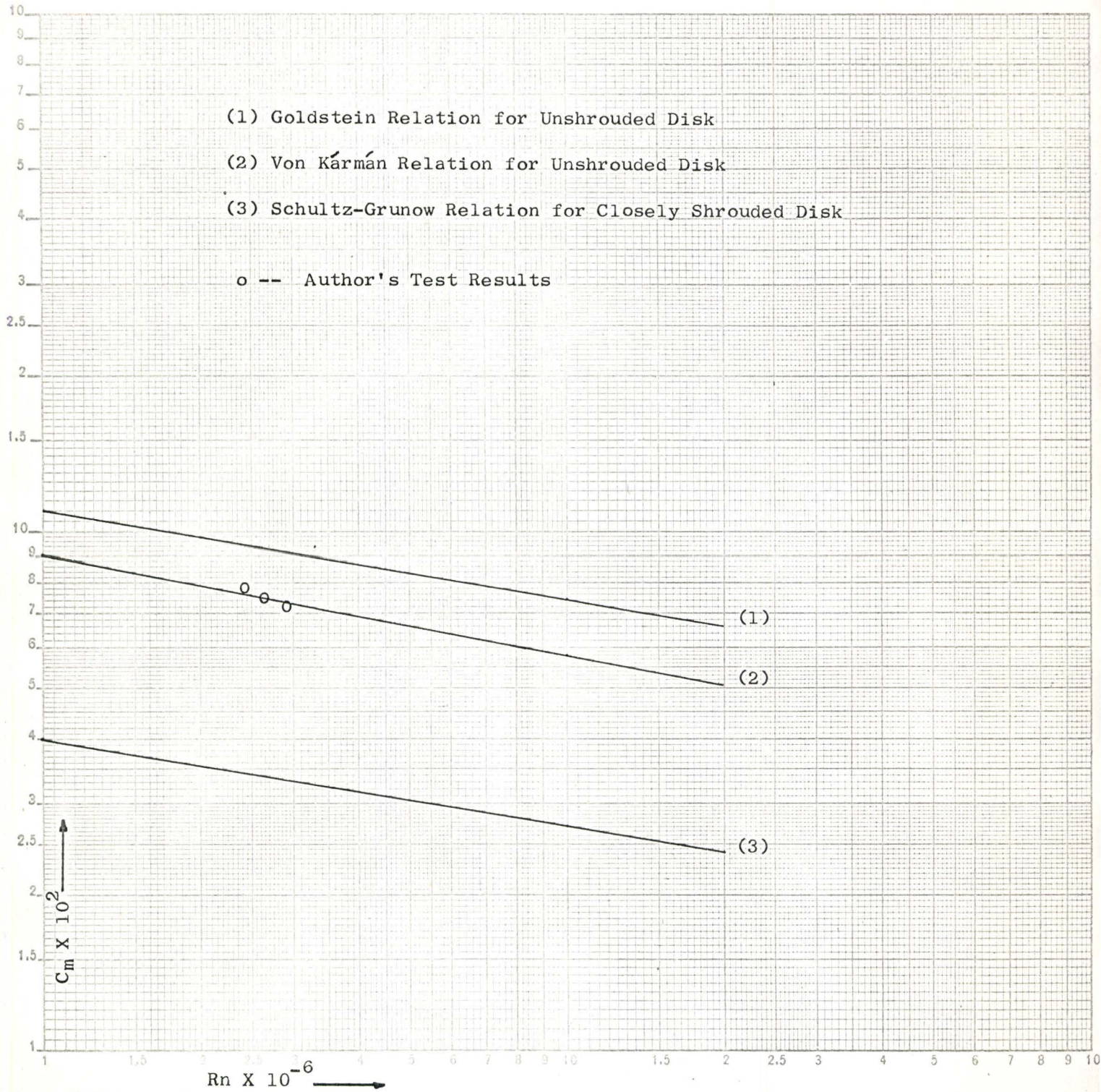

Figure 5. Moment Coefficient vs. Reynolds Number for the 10 inch diameter disk compared with shrouded and unshrouded disk relations. (Reference 9.)

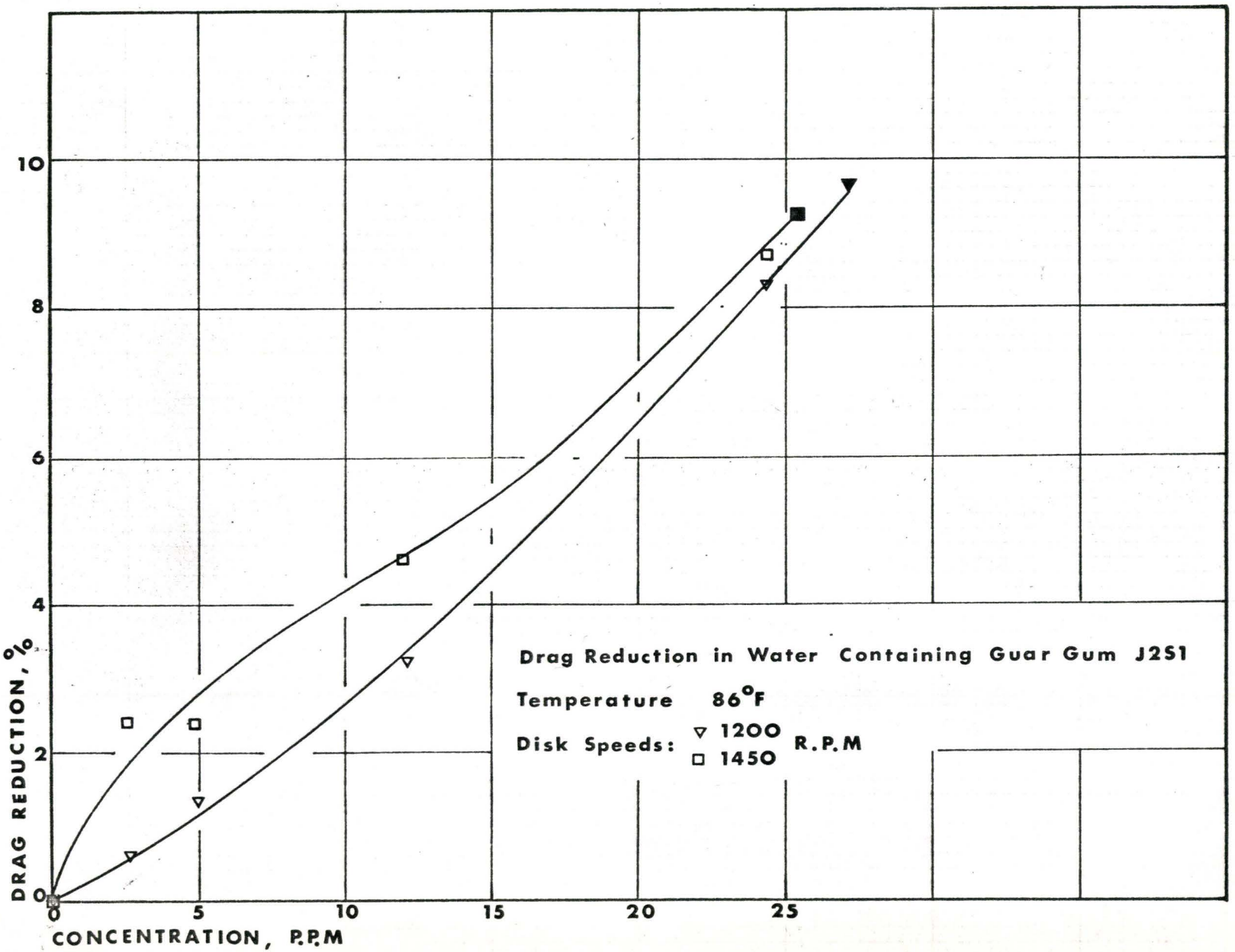
DRAG REDUCTION, %
0
2
4
6
8
10
0
5
10
15
20
25
CONCENTRATION, P.P.M
Drag Reduction in Water Containing Guar Gum J251
Temperature 86°F
Disk Speeds: ▽ 1200 R.P.M
□ 1450
Figure 6.

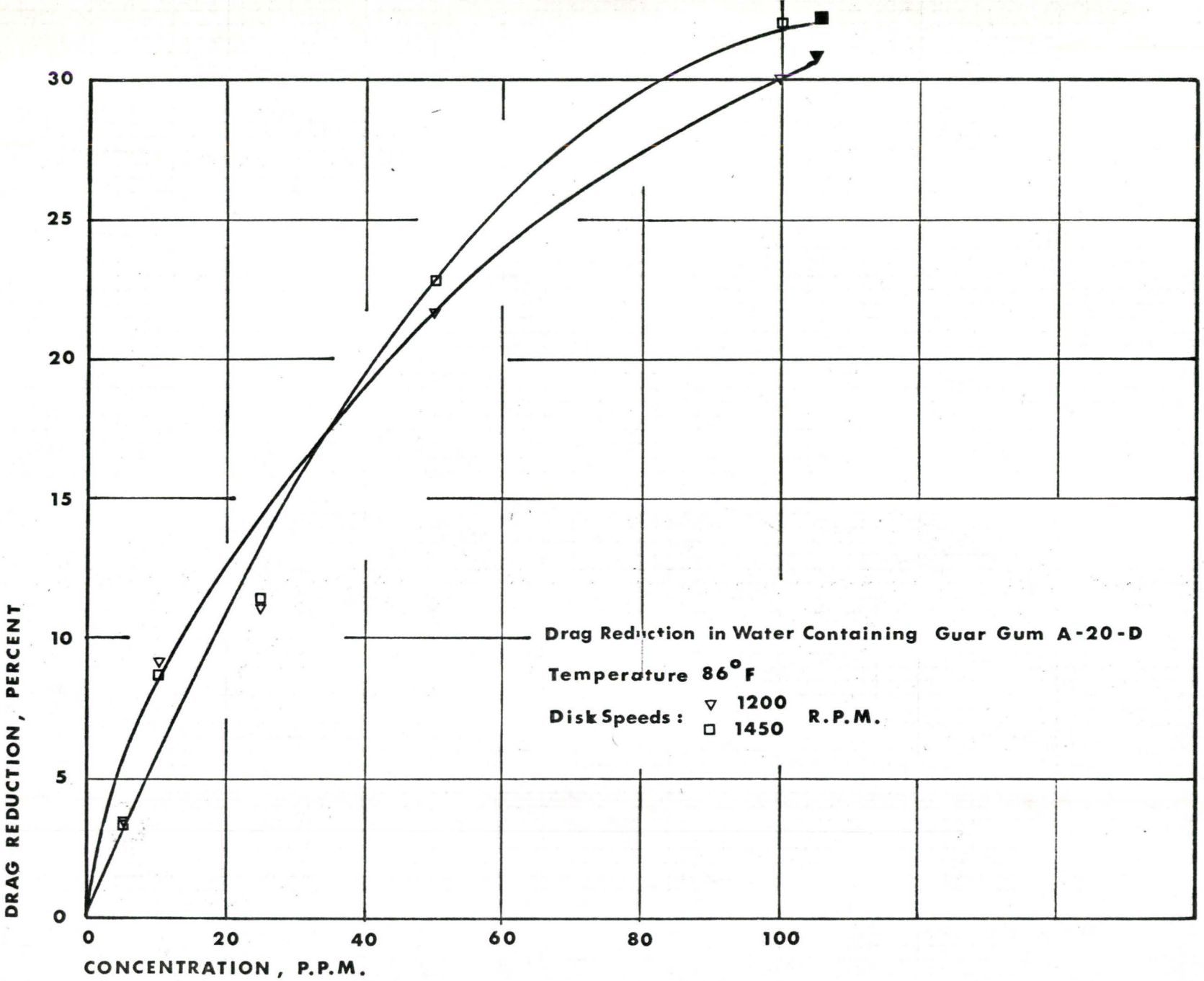
30
25
20
15
10
5
0
0
20
40
60
80
100
DRAG REDUCTION, PERCENT
CONCENTRATION, P.P.M.
Drag Reduction in Water Containing Guar Gum A-20-D
Temperature 86°F
Disk Speeds: ▽ 1200
□ 1450
R.P.M.

Figure 7.

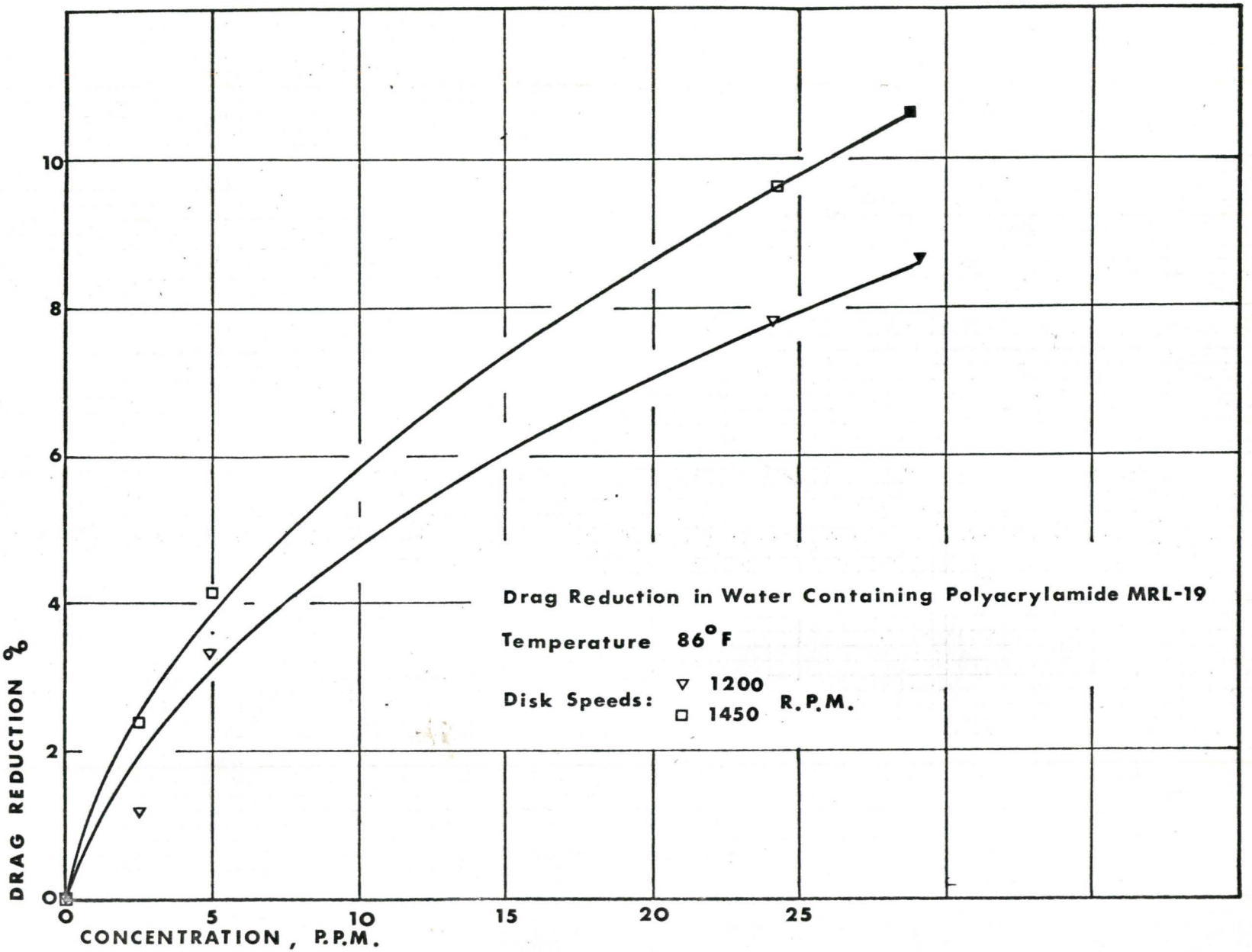
Drag Reduction in Water Containing Polyacrylamide MRL-19
Temperature 86°F
Disk Speeds: ▽ 1200 □ 1450 R.P.M.
DRAG REDUCTION %
CONCENTRATION, P.P.M.
0
2
4
6
8
10
0
5
10
15
20
25

Figure 8.

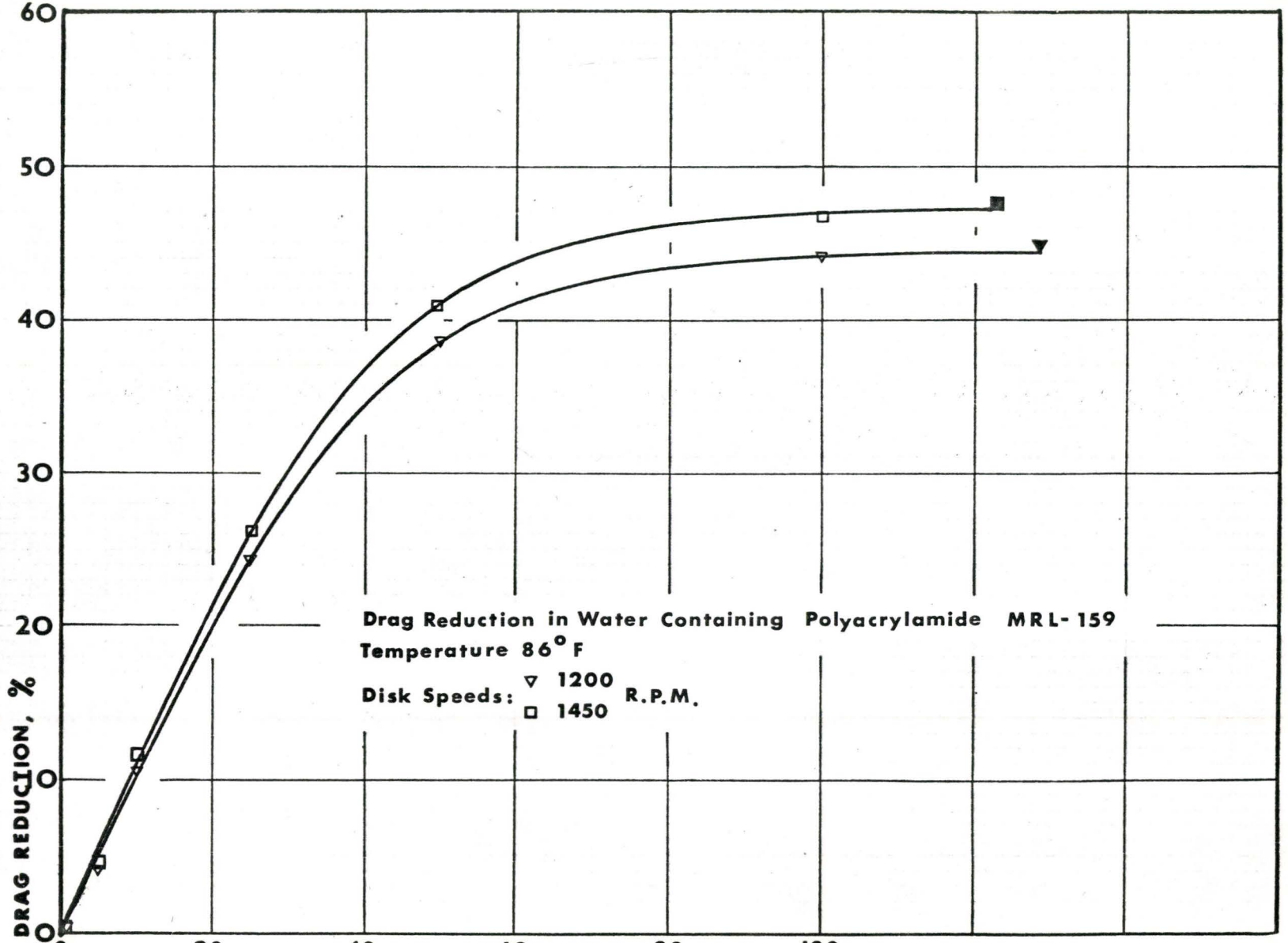
60
50
40
30
20
10
0
DRAG REDUCTION, %
0
20
40
60
80
100
CONCENTRATION, P.P.M.
Drag Reduction in Water Containing Polyacrylamide MRL-159
Temperature 86° F
Disk Speeds: ▽ 1200 R.P.M.
□ 1450
Figure 9.

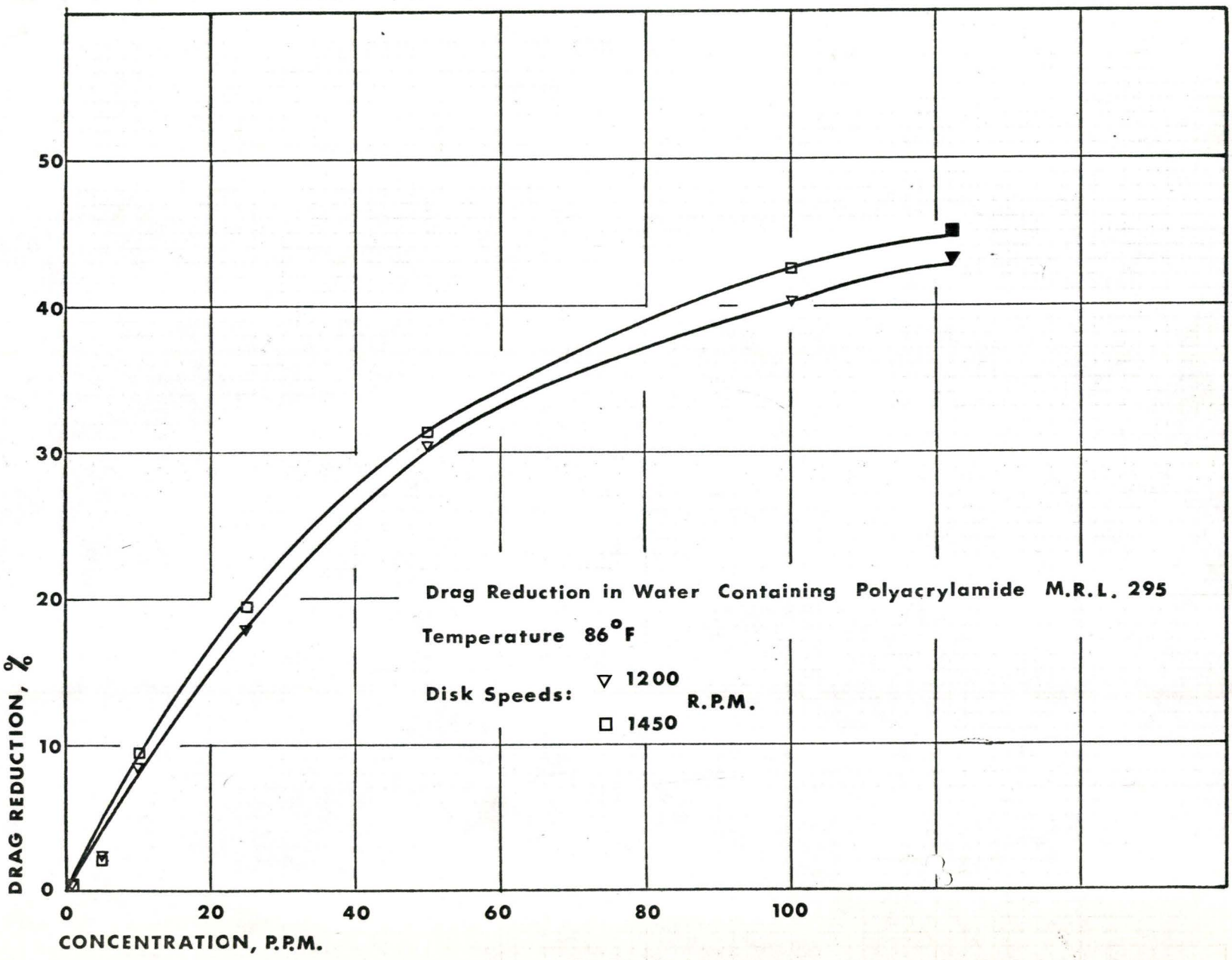
Drag Reduction in Water Containing Polyacrylamide M.R.L. 295
Temperature 86°F
Disk Speeds: ▽ 1200 R.P.M.
□ 1450
DRAG REDUCTION, %
CONCENTRATION, P.P.M.
0
10
20
30
40
50
0
20
40
60
80
100

Figure 10.

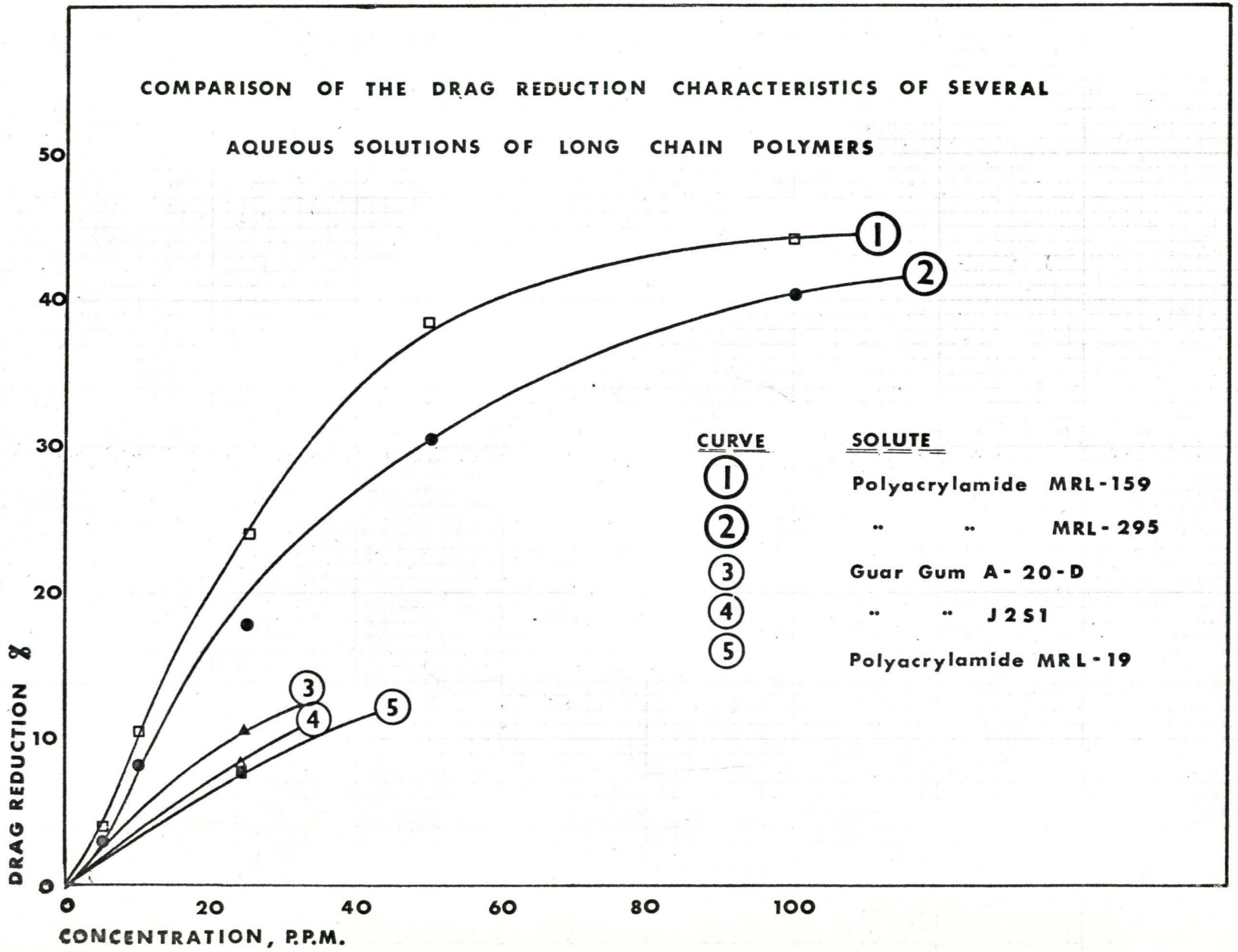
COMPARISON OF THE DRAG REDUCTION CHARACTERISTICS OF SEVERAL AQUEOUS SOLUTIONS OF LONG CHAIN POLYMERS
DRAG REDUCTION %
0
10
20
30
40
50
0
20
40
60
80
100
CONCENTRATION, P.P.M.
CURVE
SOLUTE
1 Polyacrylamide MRL-159
2 " " MRL-295
3 Guar Gum A-20-D
4 " " J251
5 Polyacrylamide MRL-19

Figure 11.

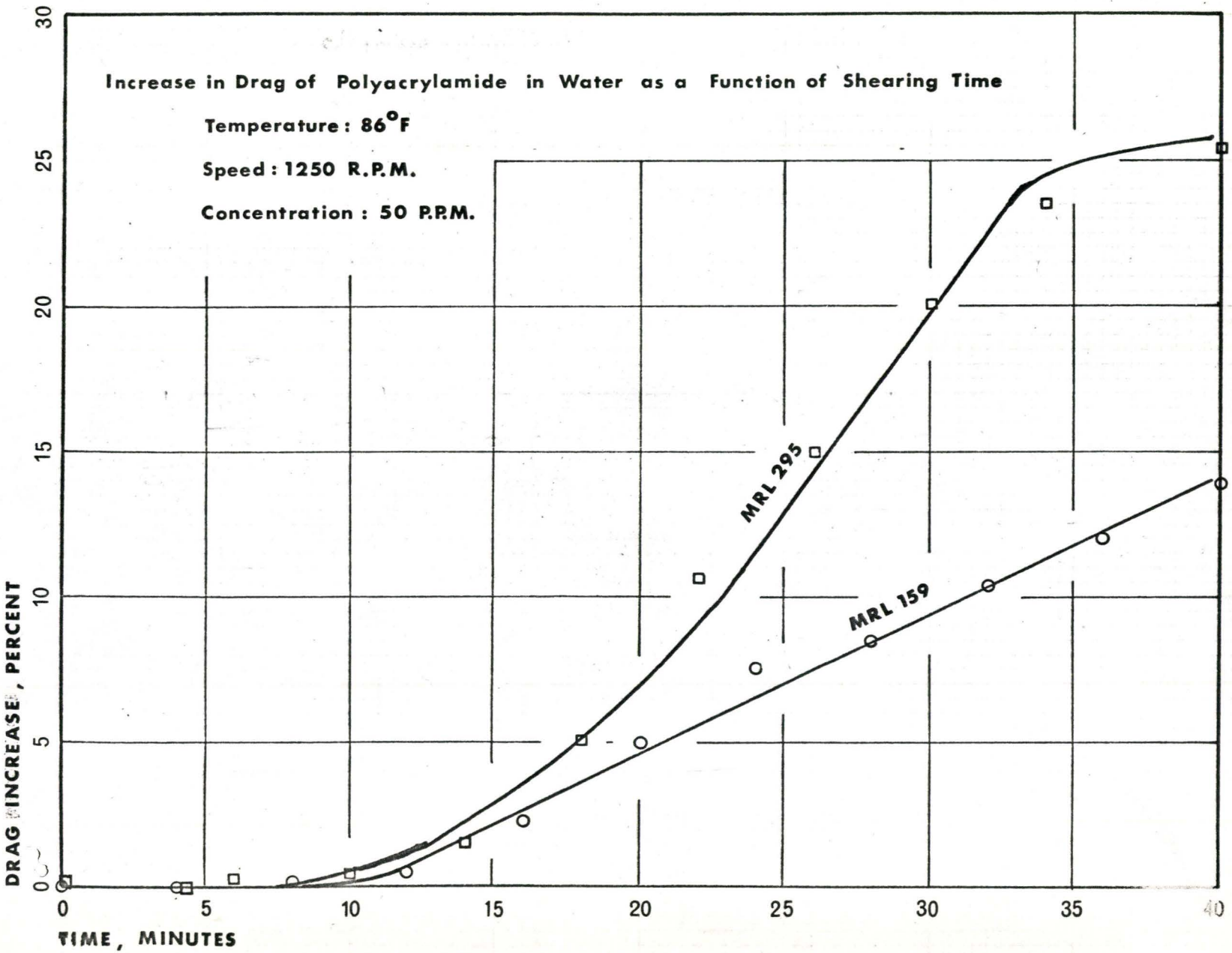
Increase in Drag of Polyacrylamide in Water as a Function of Shearing Time
Temperature : 86°F
Speed : 1250 R.P.M.
Concentration : 50 P.P.M.
MRL 295
MRL 159
DRAG INCREASE, PERCENT
TIME, MINUTES
0
5
10
15
20
25
30
35
40

Figure 12.

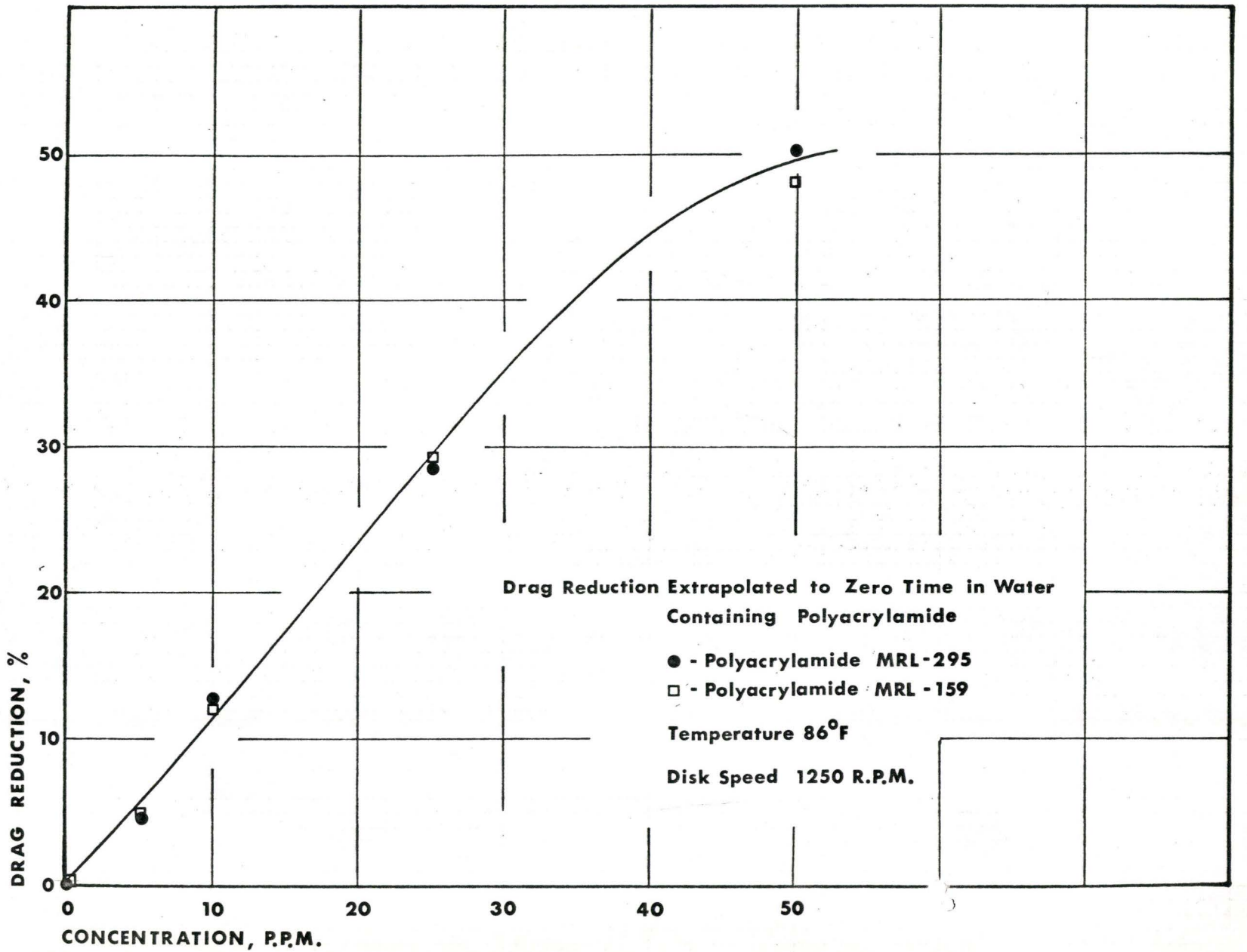
DRAG REDUCTION, %
0
10
20
30
40
50
CONCENTRATION, P.P.M.
0
10
20
30
40
50
Drag Reduction Extrapolated to Zero Time in Water Containing Polyacrylamide
● - Polyacrylamide MRL-295
□ - Polyacrylamide MRL-159
Temperature 86°F
Disk Speed 1250 R.P.M.

Figure 13.

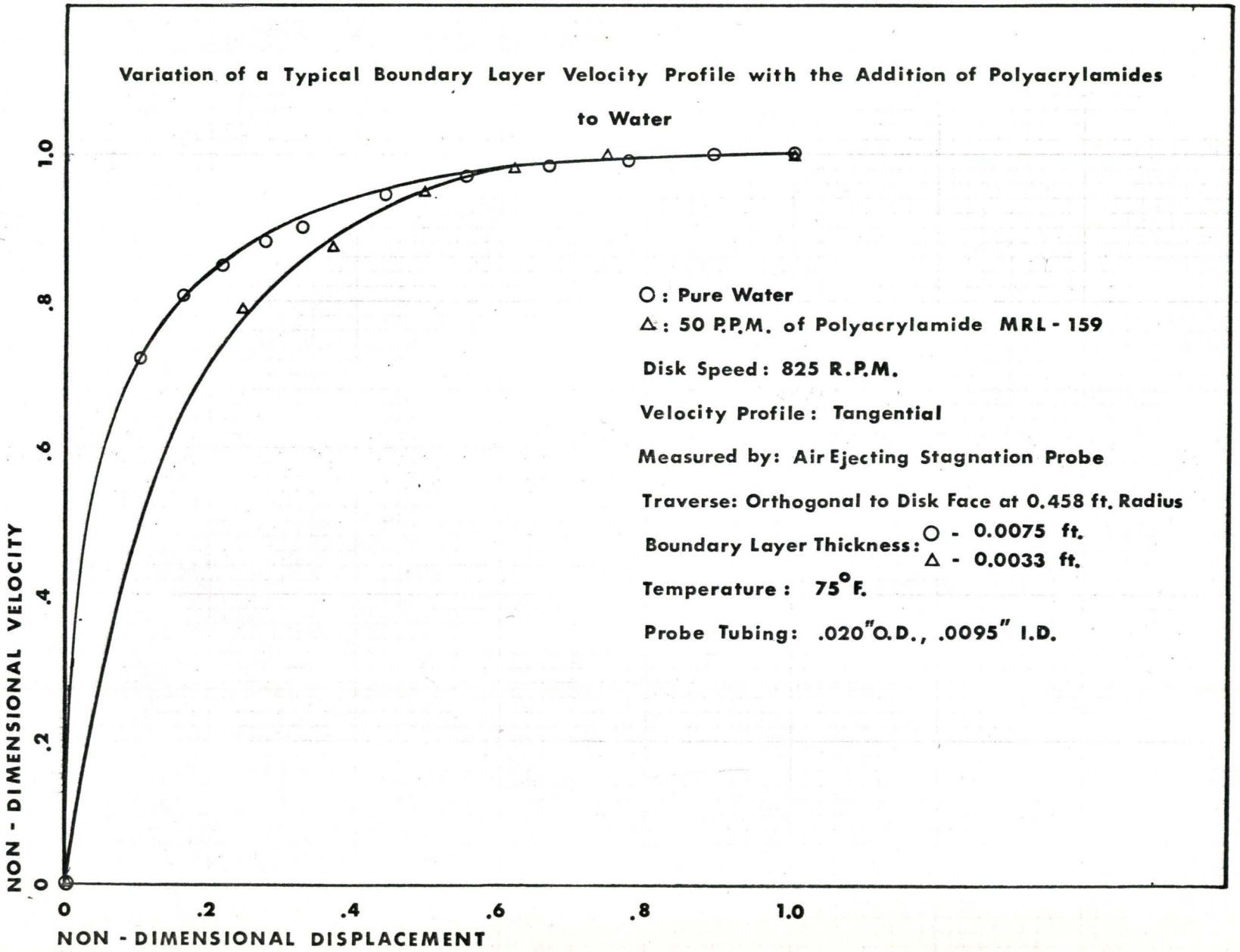
Variation of a Typical Boundary Layer Velocity Profile with the Addition of Polyacrylamides to Water
O : Pure Water
Δ : 50 P.P.M. of Polyacrylamide MRL - 159
Disk Speed : 825 R.P.M.
Velocity Profile : Tangential
Measured by: Air Ejecting Stagnation Probe
Traverse: Orthogonal to Disk Face at 0.458 ft. Radius
Boundary Layer Thickness: O - 0.0075 ft.
Δ - 0.0033 ft.
Temperature : 75° F.
Probe Tubing: .020" O.D., .0095" I.D.
NON - DIMENSIONAL VELOCITY
0
.2
.4
.6
.8
1.0
NON - DIMENSIONAL DISPLACEMENT
Figure 14.

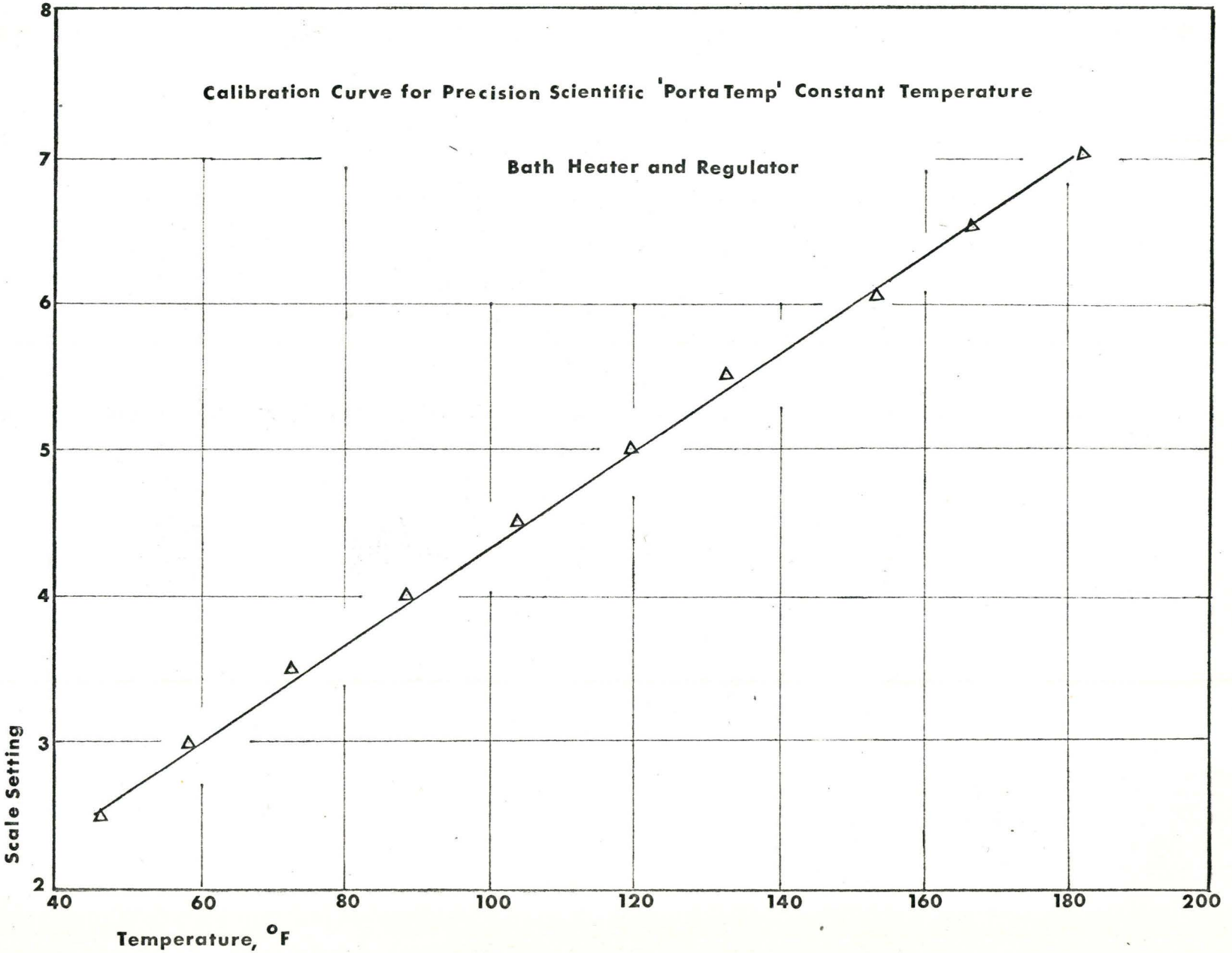
Calibration Curve for Precision Scientific 'Porta Temp' Constant Temperature
Bath Heater and Regulator
Scale Setting
Temperature, °F
8
7
6
5
4
3
2
40
60
80
100
120
140
160
180
200

Figure 15.

Velocity Probe Tip, Cross Sectional View

Scale, 10 : 1 Dimensions in Inches Joints Soldered

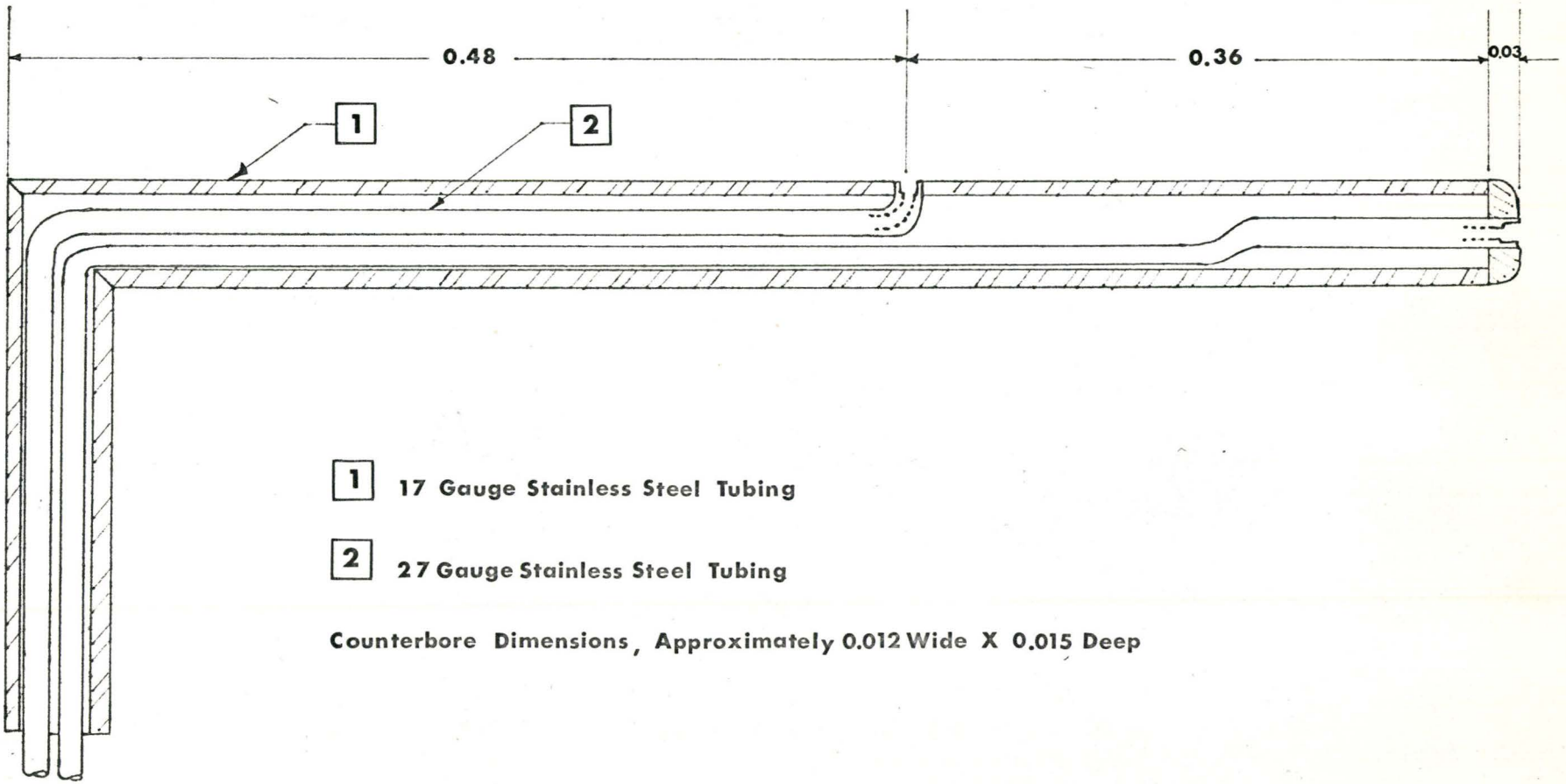

Figure 16.

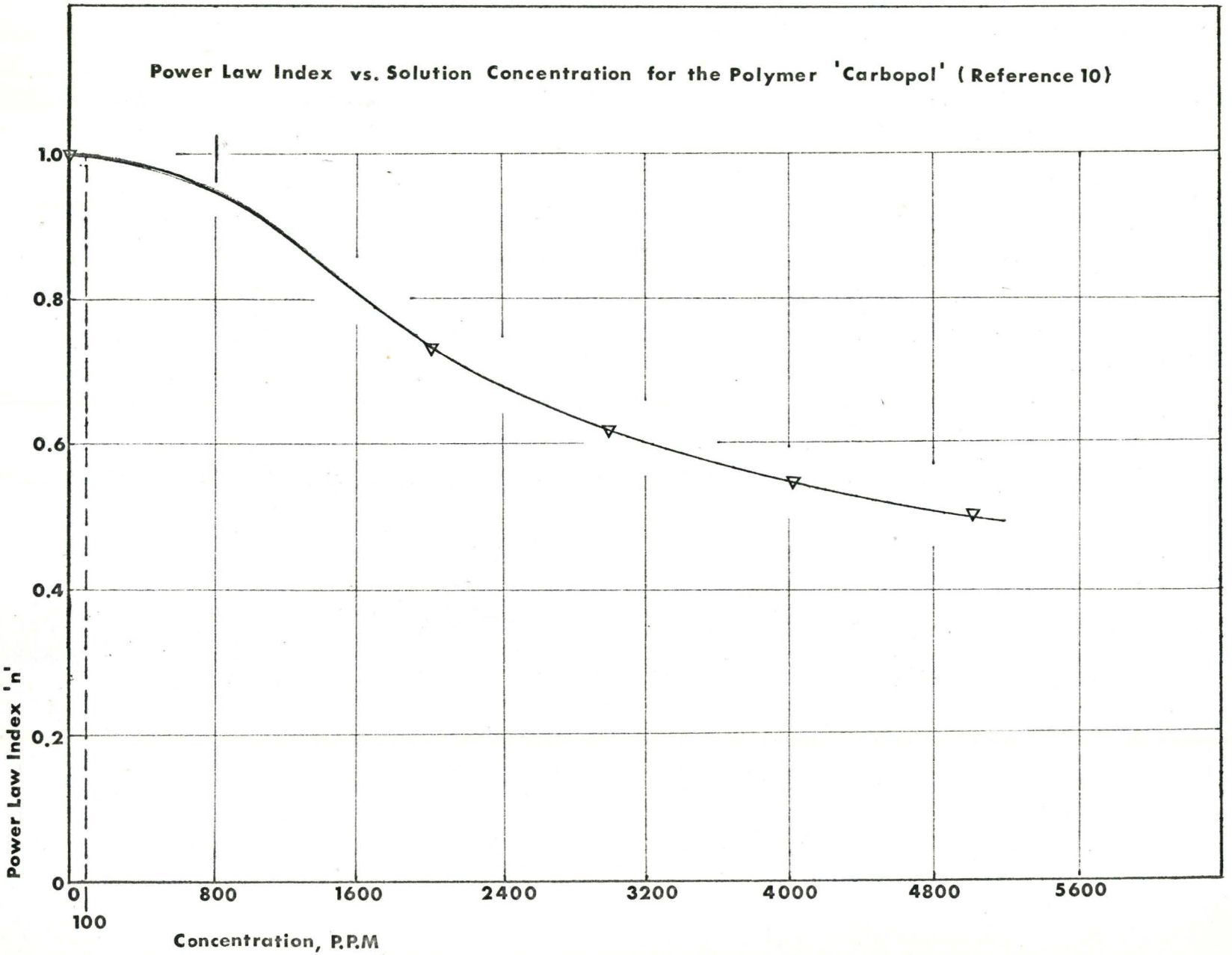
Power Law Index vs. Solution Concentration for the Polymer 'Carbopol' (Reference 10)
Power Law Index 'n'
1.0
0.8
0.6
0.4
0.2
0
0
100
800
1600
2400
3200
4000
4800
5600
Concentration, P.P.M

Figure 17.

SECTION A. TABULATED RESULTS

SPEED (R.P.M.)	TORQUE IN FT.-LBS. FOR THE POLYMER CONCENTRATIONS SHOWN BELOW.				
	0 P.P.M.	2.43 P.P.M.	4.86 P.P.M.	12.2 P.P.M.	24.3 P.P.M.
1200	1.394	1.385	1.376	1.349	1.278
1250	1.503	1.486	1.480	1.446	1.385
1300	1.608	1.586	1.577	1.549	1.476
1350	1.701	1.660	1.658	1.621	1.548
1400	1.807	1.765	1.764	1.727	1.649
1450	1.939	1.892	1.893	1.850	1.770

SPEED (R.P.M.)	DRAG REDUCTION IN PERCENT FOR THE POLYMER CONCENTRATIONS SHOWN BELOW.				
	0 P.P.M.	2.43 P.P.M.	4.86 P.P.M.	12.2 P.P.M.	24.3 P.P.M.
1200	0.0	0.65	1.29	3.23	8.32
1250	0.0	1.13	1.53	3.79	7.85
1300	0.0	1.37	1.93	3.67	8.21
1350	0.0	2.41	2.53	4.70	9.00
1400	0.0	2.32	2.38	4.43	8.74
1450	0.0	2.42	2.37	4.59	8.72

Table I. Drag Test Evaluation Record for Guar Bean Gum J2-S1.

SPEED (R.P.M.)	TORQUE IN FT.-LBS. FOR THE POLYMER CONCENTRATIONS SHOWN BELOW.			
	0 P.P.M.	2.43 P.P.M.	4.86 P.P.M.	24.3 P.P.M.
1200	1.368	1.352	1.322	1.262
1250	1.468	1.447	1.415	1.350
1300	1.570	1.550	1.516	1.437
1350	1.670	1.641	1.612	1.513
1400	1.772	1.744	1.711	1.612
1450	1.909	1.862	1.830	1.725

SPEED (R.P.M.)	DRAG REDUCTION IN PERCENT FOR THE POLYMER CONCENTRATIONS SHOWN BELOW.			
	0 P.P.M.	2.43 P.P.M.	4.86 P.P.M.	24.3 P.P.M.
1200	0.0	1.17	3.36	7.75
1250	0.0	1.43	3.61	8.04
1300	0.0	1.27	3.44	8.47
1350	0.0	1.73	3.47	9.40
1400	0.0	1.58	3.44	9.03
1450	0.0	2.46	4.14	9.64

Table II. Drag Test Evaluation Record for the Polyacrylamide MRL-19.

SPEED (R.P.M.).	TORQUE IN FT.-LBS. FOR THE POLYMER CONCENTRATIONS SHOWN BELOW.				
	0 P.P.M.	5.0 P.P.M.	10.0 P.P.M.	25.0 P.P.M.	50.0 P.P.M.
1200	1.373	1.317	1.228	1.039	0.845
1250	1.470	1.410	1.318	1.108	0.902
1300	1.579	1.516	1.410	1.175	0.960
1350	1.670	1.597	1.489	1.261	1.019
1400	1.782	1.706	1.591	1.337	1.072
1450	1.926	1.837	1.701	1.420	1.139

SPEED (R.P.M.)	DRAG REDUCTION IN PERCENT FOR THE POLYMER CONCENTRATIONS SHOWN BELOW.				
	0 P.P.M.	5.0 P.P.M.	10.0 P.P.M.	25.0 P.P.M.	50.0 P.P.M.
1200	0.0	4.08	10.56	24.33	38.46
1250	0.0	4.08	10.34	24.63	38.64
1300	0.0	3.99	10.70	25.59	39.20
1350	0.0	4.37	10.84	24.49	38.98
1400	0.0	4.26	10.72	24.97	39.84
1450	0.0	4.62	11.68	26.27	40.86

Table III. Drag Test Evaluation Record for the Polyacrylamide MRL-159.

SPEED (R.P.M.)	TORQUE IN FT.-LBS. FOR THE POLYMER CONCENTRATIONS SHOWN BELOW.			
	0 P.P.M.	5.0 P.P.M.	10.0 P.P.M.	25.0 P.P.M.
1200	1.382	1.349	1.266	1.135
1250	1.489	1.449	1.358	1.214
1300	1.584	1.550	1.448	1.290
1350	1.676	1.647	1.546	1.371
1400	1.786	1.761	1.637	1.454
1450	1.916	1.878	1.735	1.544

SPEED (R.P.M.)	DRAG REDUCTION IN PERCENT FOR THE POLYMER CONCENTRATIONS SHOWN BELOW.			
	0 P.P.M.	5.0 P.P.M.	10.0 P.P.M.	25.0 P.P.M.
1200	0.0	2.39	8.40	17.8
1250	0.0	2.68	8.79	18.5
1300	0.0	2.15	8.59	18.6
1350	0.0	1.73	7.75	18.2
1400	0.0	1.40	8.35	18.6
1450	0.0	1.98	9.48	19.4

Table IV. Drag Test Evaluation Record for the Polyacrylamide MRL-295.

SPEED (R.P.M.)	TORQUE IN FT.-LBS. FOR THE POLYMER CONCENTRATIONS SHOWN BELOW.					
	0 P.P.M.	5.0 P.P.M.	10.0 P.P.M.	25.0 P.P.M.	50.0 P.P.M.	100.0 P.P.M.
1200	1.467	1.415	1.330	1.303	1.149	1.017
1250	1.569	1.524	1.426	1.397	1.227	1.087
1300	1.674	1.627	1.531	1.504	1.308	1.158
1350	1.786	1.710	1.620	1.581	1.368	1.233
1400	1.914	1.830	1.720	1.680	1.465	1.294
1450	2.037	1.970	1.860	1.803	1.571	1.382

SPEED (R.P.M.)	DRAG REDUCTION IN PERCENT FOR THE POLYMER CONCENTRATIONS SHOWN BELOW.					
	0 P.P.M.	5.0 P.P.M.	10.0 P.P.M.	25.0 P.P.M.	50.0 P.P.M.	100.0 P.P.M.
1200	0.0	3.54	9.34	11.18	21.68	30.67
1250	0.0	2.87	9.11	10.96	21.80	30.72
1300	0.0	2.81	8.54	10.16	21.86	30.82
1350	0.0	4.26	9.29	11.48	23.40	30.96
1400	0.0	4.39	10.14	12.23	23.46	32.40
1450	0.0	3.29	8.69	11.49	22.88	32.16

Table V. Drag Test Evaluation Record for the Guar Gum A-20-D.

SPEED (R.P.M.)	TORQUE IN FT.-LBS. FOR THE POLYMERS AND THEIR CONCENTRATIONS SHOWN BELOW.			
	100.0 P.P.M. of MRL-159	50.0 P.P.M. of MRL-295	100.0 P.P.M. of MRL-295	0.0 P.P.M.
1200	0.822	1.024	0.876	1.470
1250	0.874	1.100	0.940	1.581
1300	0.930	1.174	0.996	1.691
1350	0.988	1.251	1.051	1.809
1400	1.048	1.336	1.126	1.932
1450	1.108	1.424	1.193	2.074

SPEED (R.P.M.)	DRAG REDUCTION IN PERCENT FOR THE POLYMERS AND CONCENTRATIONS SHOWN BELOW.			
	100.0 P.P.M. of MRL-159	50.0 P.P.M. of MRL-295	100.0 P.P.M. of MRL-295	0.0 P.P.M.
1200	44.08	30.34	40.41	0.0
1250	44.72	30.42	40.54	0.0
1300	45.00	30.57	41.10	0.0
1350	45.38	30.85	41.90	0.0
1400	45.76	30.85	41.72	0.0
1450	46.58	31.34	42.48	0.0

Table VI. Drag Test Evaluation Record for High Concentration Runs of the Polyacrylamides MRL-159 and MRL-295.

CONCENTRATION (P.P.M.)	REDUCTION IN DRAG EXTRAPOLATED TO ZERO TIME FOR A DISK SPEED OF 1250 R.P.M.	
	POLYACRYLAMIDE MRL-159	POLYACRYLAMIDE MRL-295
0.0	0.0	0.0
5.0	4.98	4.68
10.0	12.24	12.79
25.0	29.33	28.50
50.0	48.04	50.42

Table VII. Drag Reduction extrapolated to Zero Time for the Polyacrylamides MRL-159 and MRL-295, using a disk speed of 1250 R.P.M., for concentrations up to 50 P.P.M.

DISK SPEED (R.P.M.)	TORQUE DUE TO DRAG, Td, (Ft.-Lbs.)	MOMENT COEFFICIENT	REYNOLDS NUMBER
1150	1.373	0.00782	2.42×10^6
1200	1.460	0.00763	2.53×10^6
1250	1.555	0.00747	2.63×10^6
1300	1.660	0.00736	2.74×10^6
1350	1.742	0.00720	2.84×10^6
1400	1.862	0.00718	2.94×10^6

Table VIII. Evaluation of Reynolds Number and Dimensionless Moment Coefficient for verification of the accuracy and precision of the Measuring Apparatus (Section 4.1 and Figure 5)

DISTANCE FROM DISK FACE (thousandths of an inch)	VELOCITY REFERRED TO FREE STREAM CONDITIONS (ft./sec.)	
	WATER	50 P.P.M. OF MRL-195
0	0	0
10	21.7	26.0
15	24.1	28.8
20	25.2	31.5
25	26.0	32.1
30	26.7	32.5
40	27.8	32.9
50	28.4	32.9
60	29.1	32.9
70	29.5	32.9
80	29.6	32.9
90	29.8	32.9
100	28.8	32.9

Table IX. Boundary Layer Velocity Profile readings, treating the disk face as a Stationary Reference.

DISTANCE FROM DISK FACE (Thousandths of an inch)	VELOCITY REFERRED TO FREE STREAM CONDITIONS	
	WATER	50 P.P.M. OF MRL-195
0	0	0
10	0.728	0.790
15	0.809	0.875
20	0.846	0.957
25	0.872	0.976
30	0.896	0.988
40	0.932	1.0
50	0.953	1.0
60	0.977	1.0
70	0.990	1.0
80	0.993	1.0
90	1.0	1.0
100	1.0	1.0

Table X. Non-Dimensional Boundary Layer Velocity Profile readings, treating the disk face as a Stationary Reference.

POLYMER SAMPLE NUMBER	POLYMER NAME AND FORMULA NUMBER	PERCENT MOISTURE BY WEIGHT
3	Polyacrylamide MRL-19	9.55
4	Guar Bean Gum J2S1	7.32
6	Polyacrylamide MRL-159	4.59
7	Polyacrylamide MRL-295	3.94
8	Guar Bean Gum A-20-D	13.0

Table XI. Moisture Content expressed in percent by weight of the polymer samples employed in the experimental work, with those polymers omitted which were not effective in reducing drag.

SECTION B. SAMPLE CALCULATIONS

1. DIMENSIONLESS MOMENT COEFFICIENT

Dimensionless Moment Coefficient = (Torque Due to Drag)/ $\left[\frac{1}{2} \times (\text{Density}) \times (\text{Disk Speed})^2 \times (\text{Expanded Disk Radius})^5\right]$

i.e. $C_d = \frac{T_d}{\frac{1}{2}\rho\omega^2 R^5}$

For the first set of values in table VII, Section A of the Appendix:

ω = 1,150 R.P.M., or 120.2 rad/sec.

T_d = 1.373 Ft.-Lbs.$_f$

$R_{(e)}$ = 0.418 Ft. (Expanded Disk Radius)

ρ = 1.93 Slugs/Ft.^{3} #

Therefore: $C_d = 1.373/(\frac{1}{2} \times 1.93 \times 120.2^2 \times 0.418^5)$

$= 0.00772$

$\underline{C_d = 0.00772}$

2. REYNOLDS NUMBER

Reynolds Number = (Expanded Disk Radius)^2 x (Disk Speed) /(Kinematic Viscosity)

i.e. $R_n = \frac{R_{(e)}^2 \times \omega}{V}$

For the first set of values in table VII, Section A of the Appendix:

ω = 1,150 R.P.M., or 120.2 Rad./Sec.

$R_{(e)}$ = 0.418 Ft.

$V = 8.7 \times 10^{-6}$ Ft.^{2}/Sec. #

Fluid Properties were extracted from Table 12, of Reference 9.

Therefore: $R_n = (0.418)^2 \times 120.2/(8.7 \times 10^{-6})$

$= 2.42 \times 10^6$

$\underline{R_n = 2.42 \times 10^6}$

3. TORQUE DUE TO DRAG

Torque Due to Drag = (Gross Dynamometer Load)x(Dynamometer Moment Arm)

-(Torque Due to Frictional Losses)

i.e. $T_d = A \times L - A \times L_o$

For the 50 P.P.M. Solution of MRL-159, with a disk speed of 1200 R.P.M.:

$A = 0.875$ Ft.

$L = 1.023$ Lbs.$_f$

$(A \times L_o) = 0.05$ Ft.-Lbs.$_f$

Therefore; $T_d = 1.023 \times 0.875 - 0.05$

$= 0.845$ Ft.-Lbs.$_f$

$\underline{T_d = 0.845 \text{ Ft.-Lbs.}_f}$

4. STOCK SOLUTION CONCENTRATION

Stock Solution Concentration = (Weight of Dry Polymer) x 10^6/(Weight of Water Added to the Polymer)

i.e. $$C_s = \frac{W_{d.p} \times 10^6}{W_{w.s}}$$

In making up the 4,000 P.P.M. Stock Solution of MRL-159:

$W_{d.p}$ = 9.07 Grams

$W_{w.s}$ = 5.0 Lbs., or 2,268 Grams

Therefore: $$C_s = \frac{9.07 \times 10^6}{2,268}$$

$$= 4,000 \text{ P.P.M.}$$

$\underline{C_s = 4,000 \text{ P.P.M.}}$

5. TEST SOLUTION CONCENTRATION

Test Solution Concentration = (Stock Solution Concentration)/ $\left[1 + \frac{\text{(Weight of Water Added to Test Solution)}}{\text{(Weight of Stock Solution Added)}}\right]$

i.e. $$C_t = \frac{C_s}{1 + W_{w.t}/W_{s.t}}$$

In making up the 25 P.P.M. Test Solution of MRL-295 from 2,000 P.P.M. Stock Solution:

C_s = 2,000 P.P.M.

$W_{w.t}$ = 98.75 Lbs.

$W_{s.t}$ = 1.25 Lbs.

Therefore: $$C_t = \frac{2,000}{1 + 98.75/1.25}$$

$$= 25 \text{ P.P.M.}$$

$\underline{C_t = 25 \text{ P.P.M.}}$

6. REDUCTION IN DRAG

Reduction in Drag = 100 x [(Torque Due to Drag of Reference Fluid) - (Torque Due to Drag of Test Fluid)] / (Torque Due to Drag of Reference Fluid)

$$\text{i.e.} \quad R.D. = \frac{T_{d(\text{reference fluid})} - T_{d(\text{test fluid})}}{T_{d(\text{reference fluid})}} \times 100\%$$

Evaluating the Reduction in Drag at 1,300 R.P.M. for a 50 P.P.M. Solution of Guar Gum A-20-D:

$$T_{d(\text{reference fluid})} = 1.674 \text{ Ft.-Lbs.}_f$$

$$T_{d(\text{test fluid})} = 1.308 \text{ Ft.-Lbs.}_f$$

Therefore:
$$R.D. = \frac{1.674 - 1.308}{1.674} \times 100\%$$

$$= 21.86\%$$

$$\underline{R.D. = 21.86\%}$$

7. INCREASE IN DRAG

Increase in Drag = 100 x [(Torque Due to Drag at Elapsed Time of n Minutes) - (Torque Due to Drag at Zero Time)] / (Torque Due to Drag at Zero Time)

$$\text{i.e.} \quad I.D. = \frac{T_{d(n)} - T_{d(o)}}{T_{d(o)}} \times 100\%$$

For a 50 P.P.M. Solution of MRL-159 after 30 minutes of shearing time at 1,250 R.P.M.:

$T_{d(n)} = 1.213$ Ft.-Lbs.$_f$

$T_{d(o)} = 1.112$ Ft.-Lbs.$_f$

Therefore: $$I.D. = \frac{1.213 - 1.112}{1.112} \times 100\%$$

$$= 9.08\%$$

I.D. = 9.08%

8. SURFACE TENSION HEAD

Surface Tension Head = 2 x (Air-Water Interface Surface Tension)/[(Specific Weight of water) x (Probe Orifice Inside Radius)]

i.e. $$h_{s.t} = \frac{2T_{s.t}}{\gamma_w \times R_p}$$

For the probe used, and for water and weak aqueous solutions as used throughout this thesis:

$R_p = 0.00475$ inches, or 0.000396 Ft.

$\gamma_w = 62.4$ Lbs.$_f$/Ft.^{3}

$T_{s.t} = 0.0052$ Lbs.$_f$/Ft. #

Therefore: $$h_{s.t} = \frac{2 \times 0.0052}{62.4 \times 0.000396}$$

$$= 0.421 \text{ Ft. or } 5.05 \text{ inches.}$$

$h_{s.t} = 5.05$ inches

Fluid Property taken from page 29 of Reference 8.

9. FLUID VELOCITY

Fluid Velocity = $\left[2 \times (\text{Acceleration Due to Gravity}) \times (\text{Velocity Head})\right]^{\frac{1}{2}}$

where: Velocity Head = Manometric Head - Hydrostatic Head - Surface Tension Head

i.e. $V_f = \left[2 \times g \times (H - h_s - h_{s.t})\right]^{\frac{1}{2}}$

Using a disk speed of 825 R.P.M., and a distance x = 50 thousandths of an inch out from the disk:

$H = 33.6$ inches of water

$h_s = 4.83$ inches of water

$h_{s.t} = 5.05$ inches of water

Therefore: $V_f = \left[2 \times 32.2 \times (33.6 - 4.83 - 5.05)\right]^{\frac{1}{2}}$

$= 11.3$ Ft./Sec. relative to the probe.

The linear velocity at a point on the disk at the probe radius is:

Velocity = (Measuring Radius) x (Disk Speed)

i.e. Velocity of Disk = $R_m \times \omega$

$R_m = 5.5$ inches, or 0.458 Ft.

$\omega = 825$ R.P.M., or 86.4 Rad./Sec.

Therefore: $V_{disk} = 0.458 \times 86.4$

$= 39.7$ Ft./Sec.

The resultant fluid velocity 50 thousandths of an inch out from the disk, relative to the disk is:

$V_{f(\text{relative to disk})} = V_{disk} - V_{f(\text{relative to probe})}$

Therefore: $V_{f(\text{relative to disk})} = 39.7 - 11.3$

$= 28.4$ Ft./Sec.

$\underline{V_{f(\text{relative to disk})} = 28.4 \text{ Ft./Sec.}}$

SECTION C. VERIFICATION OF THE FREE DISK ASSUMPTION

It can readily be seen from figure 5 that the rotating disk is operating essentially as a free disk. That is, the walls of the main chamber are far away from the disk relative to the thickness of the boundary layer which builds up on the disk.

The maximum boundary layer thickness for the ten inch diameter disk which will occur at the average disk speed of 1,300 R.P.M. occurs at the maximum radius of the disk and is given by:

$$\delta = 0.526 \times R \times (V/R^2\omega)^{1/5} \qquad \#$$

Where: δ is the boundary layer thickness in feet

R is the disk radius in feet, and is 0.417 Ft.

V is the kinematic viscosity, and is 8.7×10^{-6} Ft.^{2}/Sec.

ω is the disk speed, and is 136 Rad./Sec.

Therefore: $$\delta_{max.} = 0.526 \times 0.417 \times \left[\frac{8.7 \times 10^{-6}}{(0.417)^2 \times 136}\right]$$

$$= 0.0113 \text{ Ft.}$$

Compared with this value, the closest wall of the main chamber is approximately 0.25 Ft. away, that is, approximately twenty-two boundary layer thicknesses distant.

Furthermore, the spacing to disk radius ratio used was approximately 0.67 on one side of the disk, and 1.4 on the other side. Disks with a spacing to radius ratio of 0.217 on both

---

\# Relation taken from p. 548, equation 21-26 of reference 9.

sides show themselves to be only 50% shrouded in terms of Dimensionless Moment Coefficient vs. Reynolds Number relations (16). Considering that the test data of Dimensionless Moment Coefficient vs. Reynolds Number lie between or near the Von Kármán and Goldstein relations, we can say that our disk is operating under essentially unshrouded conditions.

SECTION D. CALCULATION OF THE HYPOTHETICAL REYNOLDS NUMBER PREDICTED BY THE TRANSITION OFFSET THEORY, AND THE BASIS FOR THE REJECTION OF THE THEORY.

(i) Calculation of Laminar Drag Torque for an Unshrouded Disk.

Using the relationships:

$$C_m = 3.870\ R_n^{-\frac{1}{2}} \qquad \#$$

$$C_m = T_d / \tfrac{1}{2} \rho \omega^2 R^5$$

$$R_n = R^2 \omega / V$$

We can combine them to form:

$$\underline{T_d = 1.935 \times V^{\frac{1}{2}} \times \omega^{\frac{3}{2}} \times R^4 \times \rho}$$

(ii) Calculation of Turbulent Drag Torque for an Unshrouded Disk:

Using the relationships:

$$C_m = 0.146\ R_n^{-\frac{1}{5}} \qquad \#\#$$

$$C_m = T_d / \tfrac{1}{2} \rho \omega^2 R^5$$

$$R_n = R^2 \omega / V$$

We can combine them to form:

$$T_d = 0.073 \times \rho \times \omega^{9/5} \times R^{23/5} \times V^{1/5}$$

(iii) Substituting the following values determined in the velocity profile tests:

ω = 825 R.P.M., or 86.4 Rad./Sec., ρ = 1.932 Slugs/Ft.^{3}

$V = 9.8 \times 10^{-6}$ Ft.^{2}/Sec. ###

Values annoted above were taken from reference 9 as follows:

\# -- p. 546, equation 21-23. ## -- p. 548, equation 21-25,

-- p. 8, table 12.

The expression for Laminar Drag Torque becomes:

$$T_d = 9.55\ R^4 \quad \text{Ft.-Lbs.}_f$$

The expression for Turbulent Drag Torque becomes:

$$T_d = 42.5\ R^{4.6} \quad \text{Ft.-Lbs.}_f$$

(iv) To Determine the Applicable Drag Torque:

$T_{d(\text{effective})}$ = T_d laminar, for the range of R_n from 0 to R_n transition

+ T_d turbulent, for the range of R_n from 0 to R_n maximum

- T_d turbulent, for the range of R_n from 0 to R_n transition.

For water, the transition Reynolds Number is 3×10^5. #

Using the relationship $R = (\nu \times R_n/\omega)^{\frac{1}{2}}$ to evaluate the transition radius for pure water we get:

$$R_{\text{transition}} = \left(\frac{9.8 \times 10^{-6} \times 3 \times 10^5}{86.4}\right)^{\frac{1}{2}}$$

$$= 0.1845 \text{ Ft.}$$

Thus for water, using the relation for Drag Torque from part (iv) above we get:

$$T_d \text{ effective} = 9.55 \times (0.1845)^4 + 42.5 \times (0.5)^{4.6} - 42.5 \times (0.1845)^{4.6}$$

From which $\underline{T_d \text{ effective} = 1.74 \text{ Ft.-Lbs.}_f}$

Value taken from p. 88 of reference 9.

(v) Calculation of Transition Radius Based on the Transition Offset Theory.

The drag reduction of the 50 P.P.M. solution of the polymer MRL-159 used in the velocity profile determination tests was 29.8%. Using an iterative procedure we find a transition radius which will account for this drag reduction, i.e. for which the drag torque is:

T_d = (100-29.8)% of T_d effective of pure water,

= 1.22 Ft.-Lbs.$_f$

At a transition radius of 0.425 Ft., or 5.1 inches,

$$T_d \text{ effective} = 9.55 \times (0.425)^4 + 42.5 \times (0.5)^{4.6} - 42.5 \times (0.425)^{4.6}$$

$$= 1.22 \text{ Ft.-Lbs.}_f$$

On the basis of the Turbulent Suppression Theory, a transition to fully turbulent flow should occur at a radius of 5.1 inches. However, non-fully turbulent profiles were observed to occur at a greater radius, namely 5.5 inches; hence, we can reject the Transition Offset Theory.